

Assessing the Impact of Hydrogen Absorption on the Characteristics of the Galactic Center Excess



Oscar Macias

with M. Pohl (DESY), P. Coleman (UofC), C. Gordon (UofC)

ApJ 929 (2022) 2, 136 [arXiv:2203.11626]

IDM 2022,

Technical University Vienna

The Fermi GeV Excess

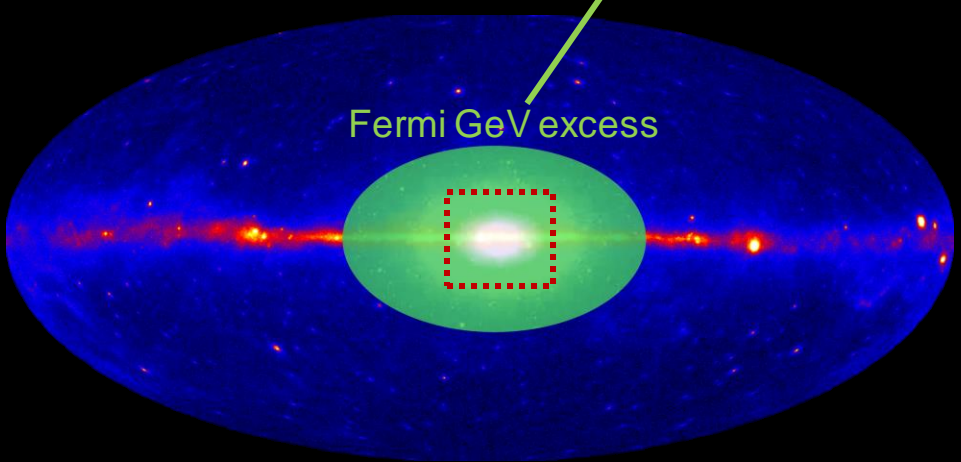
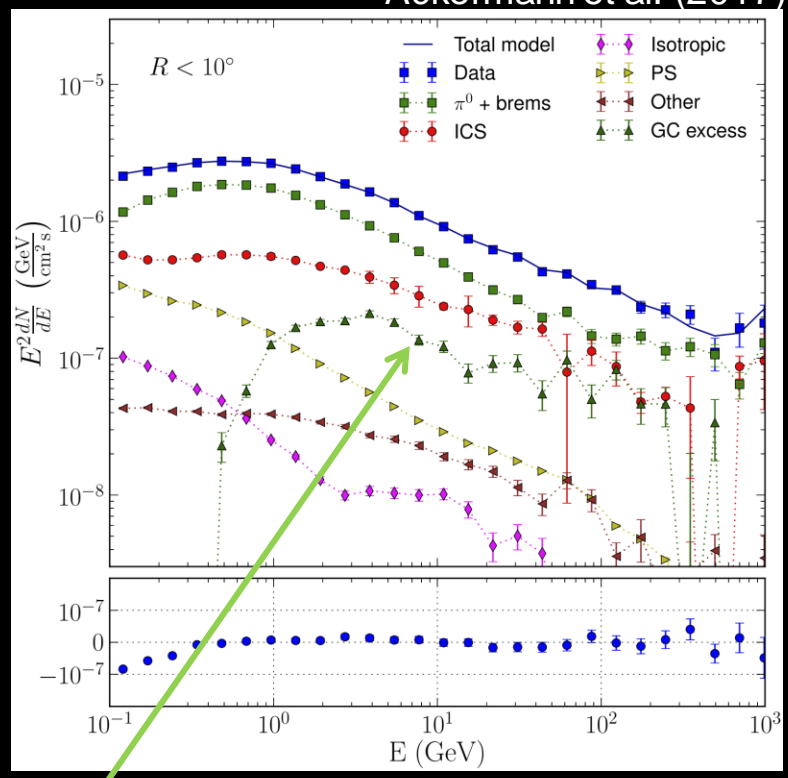
Ackermann et al. (2017)

At the Galactic Center

- Goodenough & Hooper (2009)
- Vitale & Morselli (2009)
- Hooper & Goodenough (2011)
- Hooper & Linden (2011)
- Boyarsky et al (2011)
- Abazajian & Kaplinghat (2012)
- Gordon & Macias (2013)
- Macias & Gordon (2014)
- Abazajian et al (2014, 2015)
- Calore et al (2014)
- Daylan et al (2014)
- Selig et al (2015)
- Huang et al (2015)
- Gaggero et al (2015)
- Carlson et al (2015, 2016)
- de Boer et al (2016)
- Yang & Aharonian (2016)
- Fermi Coll. (2016)
- Horiuchi et al (2016)
- Linden et al (2016)
- Ackermann et al (2017)
- Macias et al (2018)
- Bartels et al (2018)
- Balaji et al (2018)
- Zhong et al (2019)
- Macias et al (2019)
- Chang et al (2020)
- Buschmann et al (2020)
- Leane & Slatyer (2020)
- Abazajian et al (2020)
- List et al (2020)
- Di Mauro (2020)
- Burns et al (2020)
- Cholis et al (2022)
- Pohl, Macias+(2022)
- ...

At mid-lat

- Hooper & Slatyer (2013)
- Huang et al (2013)
- Zhou et al (2014)
- Daylan et al (2014)
- Calore et al (2014)
- ...



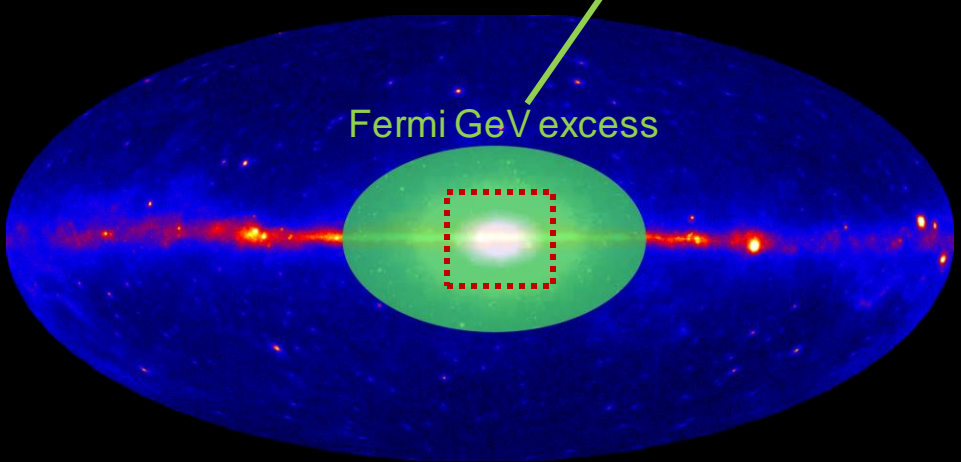
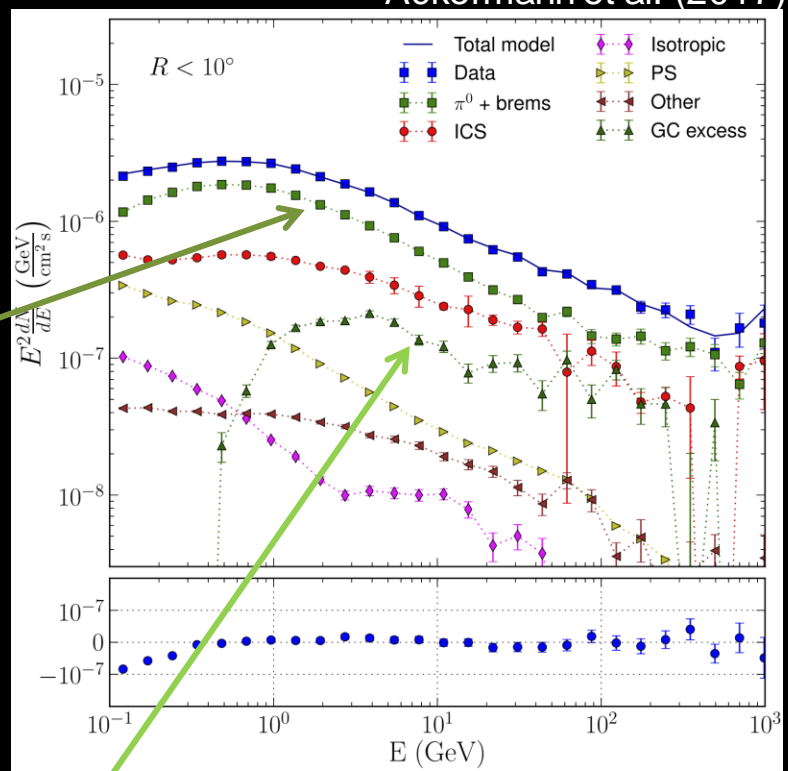
The Fermi GeV Excess

Ackermann et al. (2017)

At the Galactic Center

- Goodenough & Hooper (2009)*
- Vitale & Morselli (2009)*
- Hooper & Goodenough (2011)*
- Hooper & Linden (2011)*
- Boyarsky et al (2011)*
- Abazajian & Kaplinghat (2012)*
- Gordon & Macias (2013)*
- Macias & Gordon (2014)*
- Abazajian et al (2014, 2015)*
- Calore et al (2014)*
- Daylan et al (2014)*
- Selig et al (2015)*
- Huang et al (2015)*
- Gaggero et al (2015)*
- Carlson et al (2015, 2016)*
- de Boer et al (2016)*
- Yang & Aharonian (2016)*
- Fermi Coll. (2016)*
- Horiuchi et al (2016)*
- Linden et al (2016)*
- Ackermann et al (2017)*
- Macias et al (2018)*
- Bartels et al (2018)*
- Balaji et al (2018)*
- Zhong et al (2019)*
- Macias et al (2019)*
- Chang et al (2020)*
- Buschmann et al (2020)*
- Leane & Slatyer (2020)*
- Abazajian et al (2020)*
- List et L (2020)*
- Di Mauro (2020)*
- Burns et al (2020)*
- Cholis et al (2022)*
- Pohl, Macias+(2022)*
- ...
- Hooper & Slatyer (2013)*
- Huang et al (2013)*
- Zhou et al (2014)*
- Daylan et al (2014)*
- Calore et al (2014)*
- ...

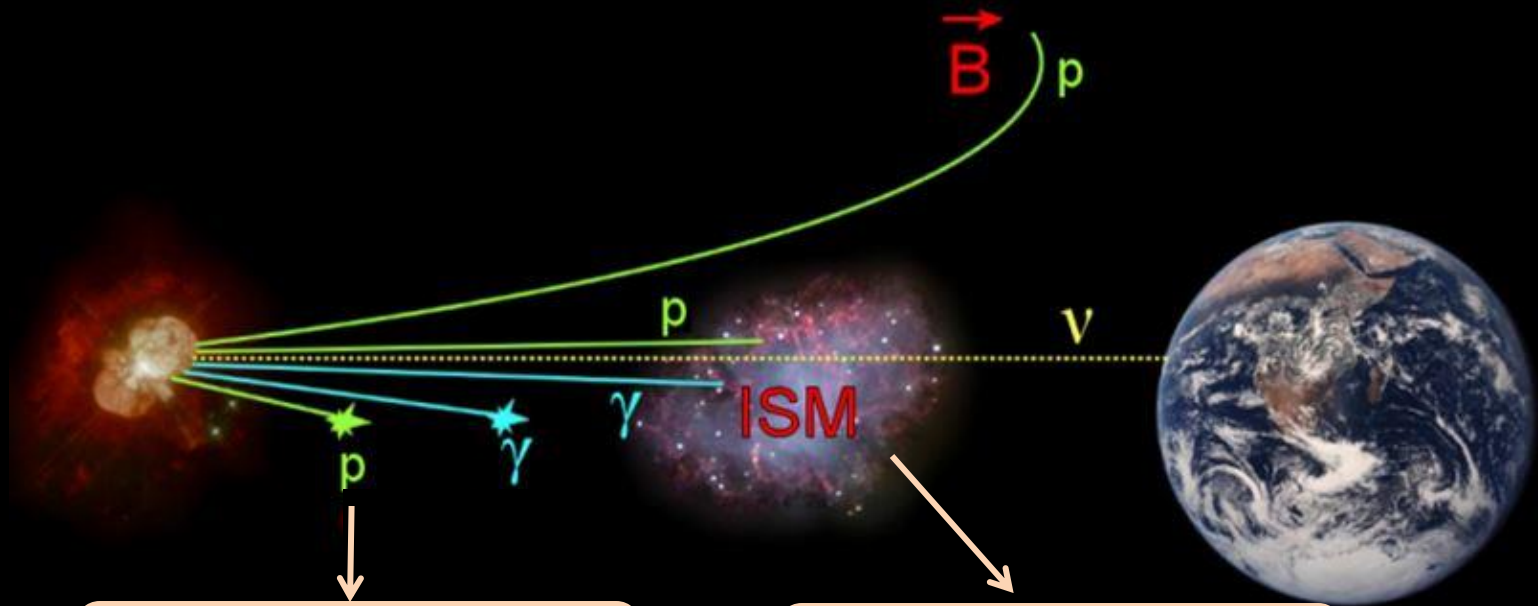
Gas-correlated
gamma rays
dominate in this
sky region



At mid-lat

- Hooper & Slatyer (2013)*
- Huang et al (2013)*
- Zhou et al (2014)*
- Daylan et al (2014)*
- Calore et al (2014)*
- ...

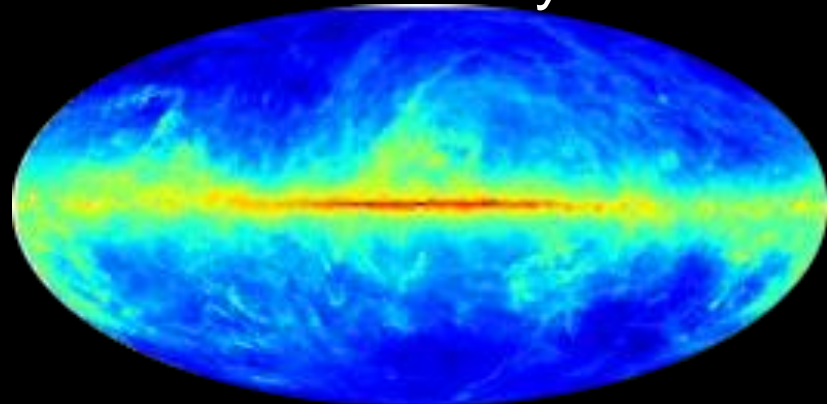
Ingredients of the Gas-correlated emission



Cosmic Ray Densities

Interstellar Gas

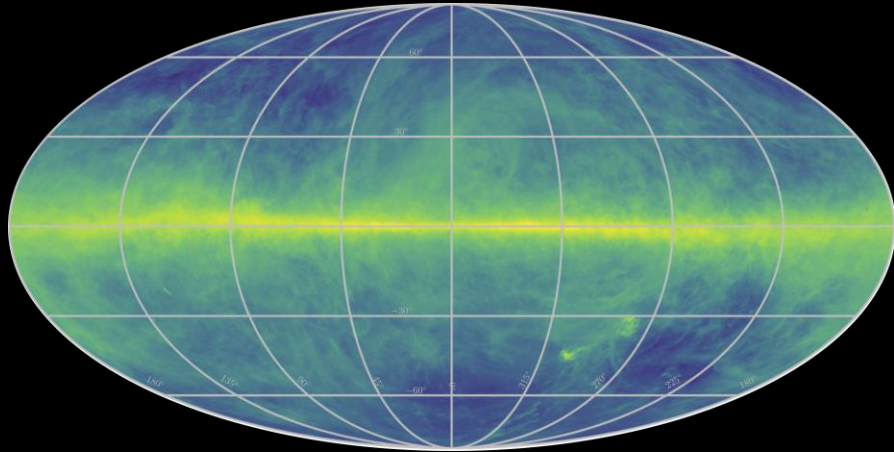
Gamma rays



See Mattia's and Ilias' talks!

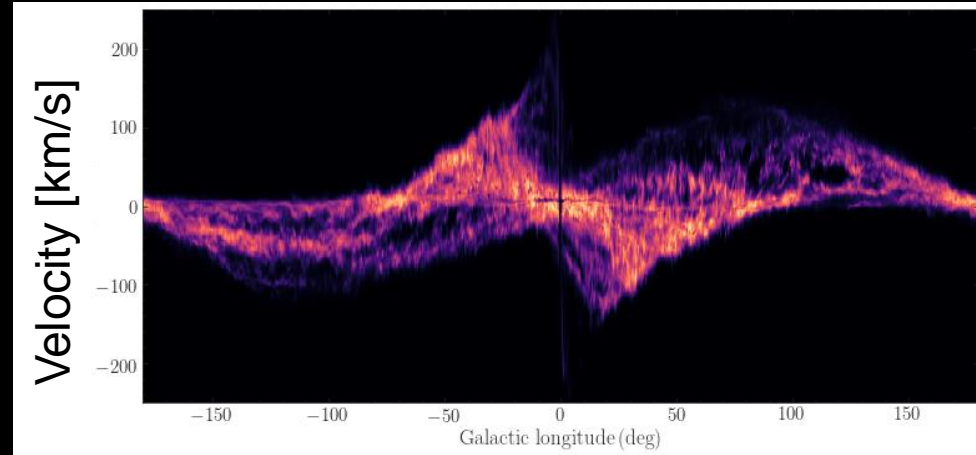
Interstellar Hydrogen Measurements

HI4PI survey, Ben Bekhti et al. (2016)



Total hydrogen column density

J. Bovy (2021)



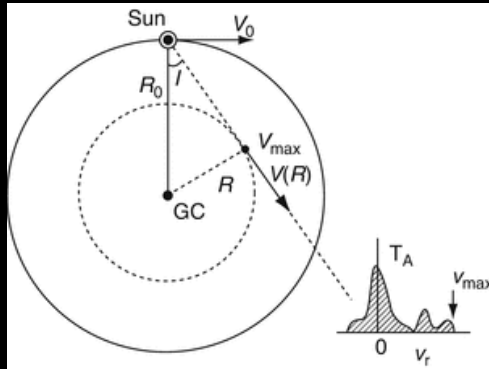
Line-of-sight HI velocity

➔ What is needed is the spatial distribution of hydrogen along the line of sight

Constructing the new hydrogen maps

Previous approach

- Assumes circular motion of hydrogen gas (interpolation method)

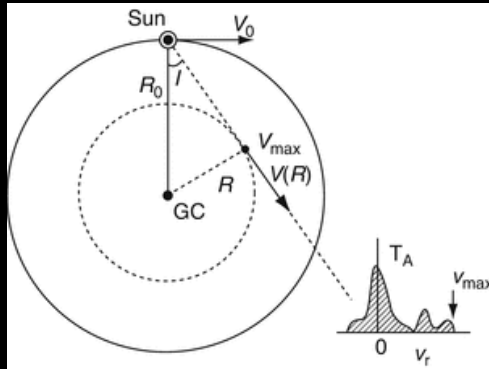


Circular orbits of gas

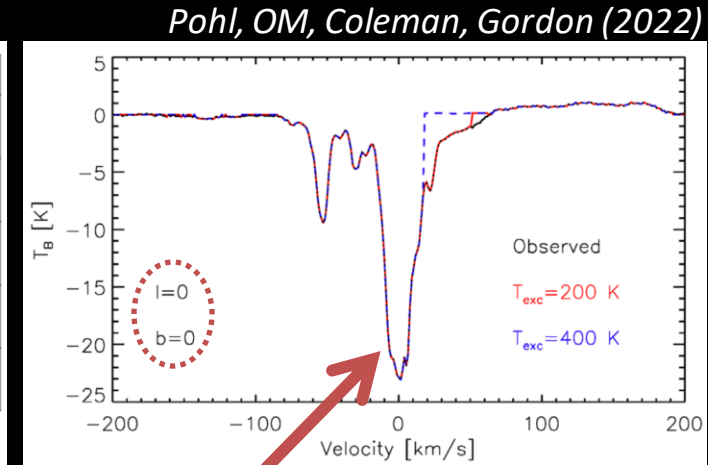
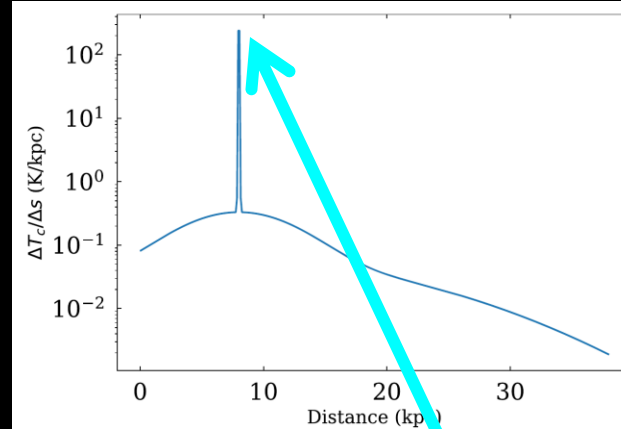
Constructing the new hydrogen maps

Previous approach

- Assumes circular motion of hydrogen gas (interpolation method)
- Disregards continuum emission and absorption.



Circular orbits of gas

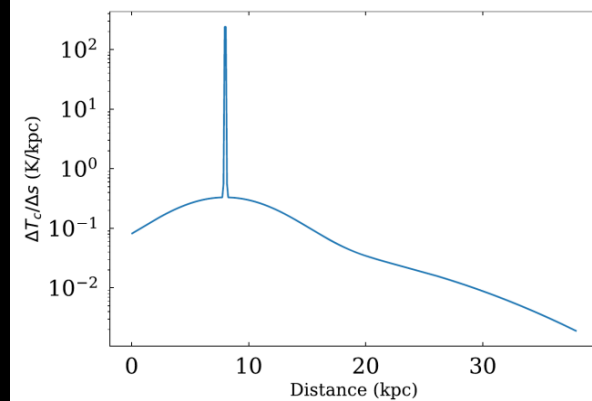
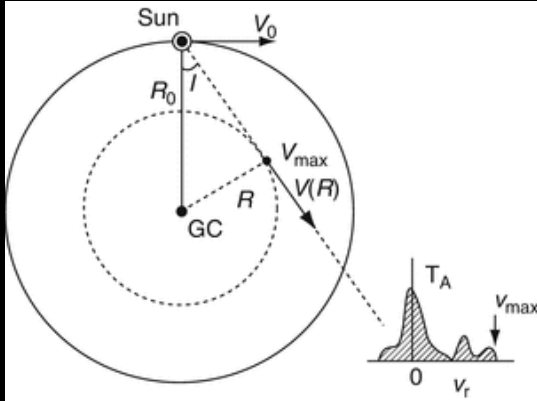


Strong **continuum** and **absorption** features @ GC

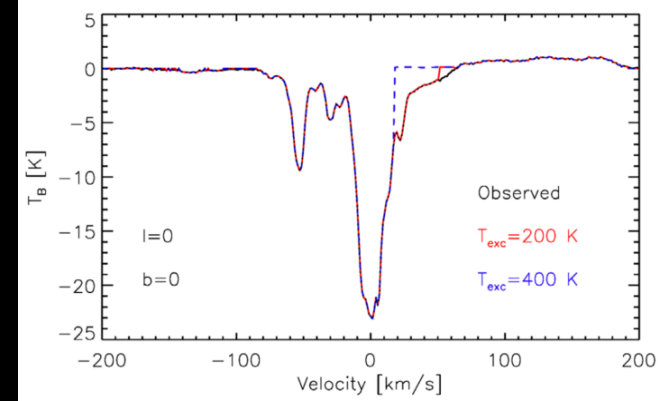
Constructing new hydrogen maps

Previous approach

- Assumes circular motion of hydrogen gas (interpolation method)
- Disregards continuum emission and absorption.

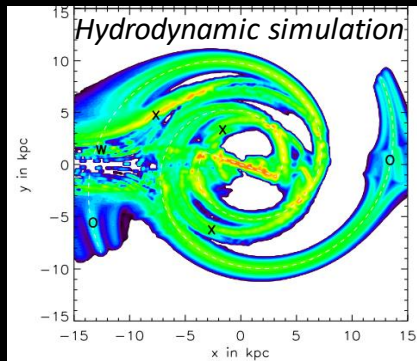


Pohl, OM, Coleman, Gordon (2022)



New approach

- Gas-flow model from hydrodynamic simulations
- Solve the radiative transfer equation



Pohl+ (2009)

Line emission

$$\frac{dI}{ds} = j_c + j_l - \alpha_l I$$

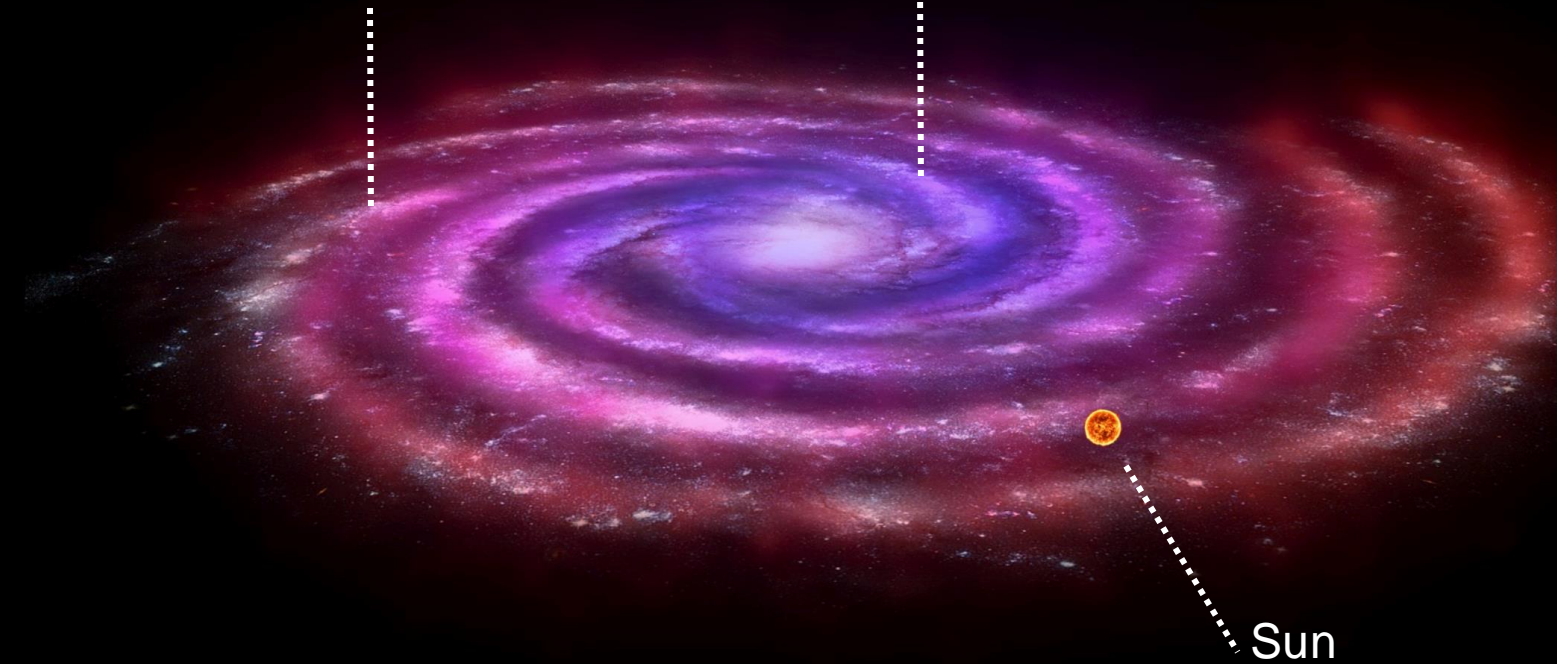
Continuum emission Absorption

Modeling Strategy: gas maps divided in rings

Atomic hydrogen

Molecular hydrogen

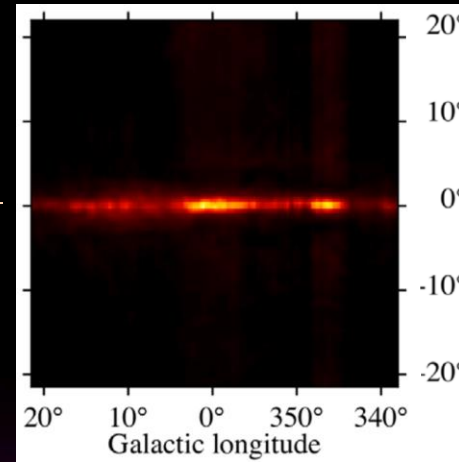
Sun



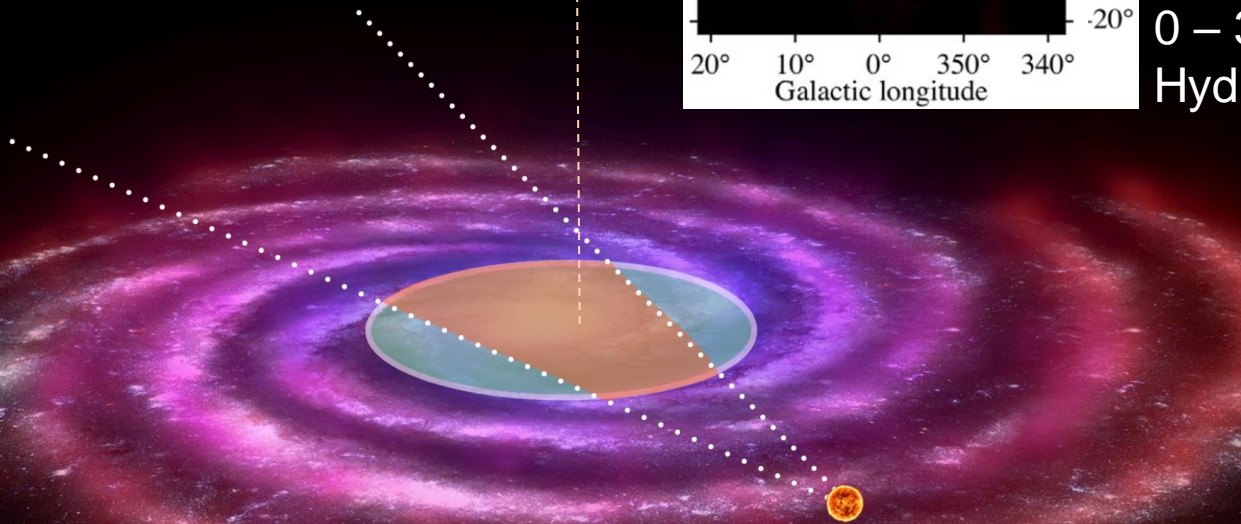
Modeling Strategy: gas maps divided in rings



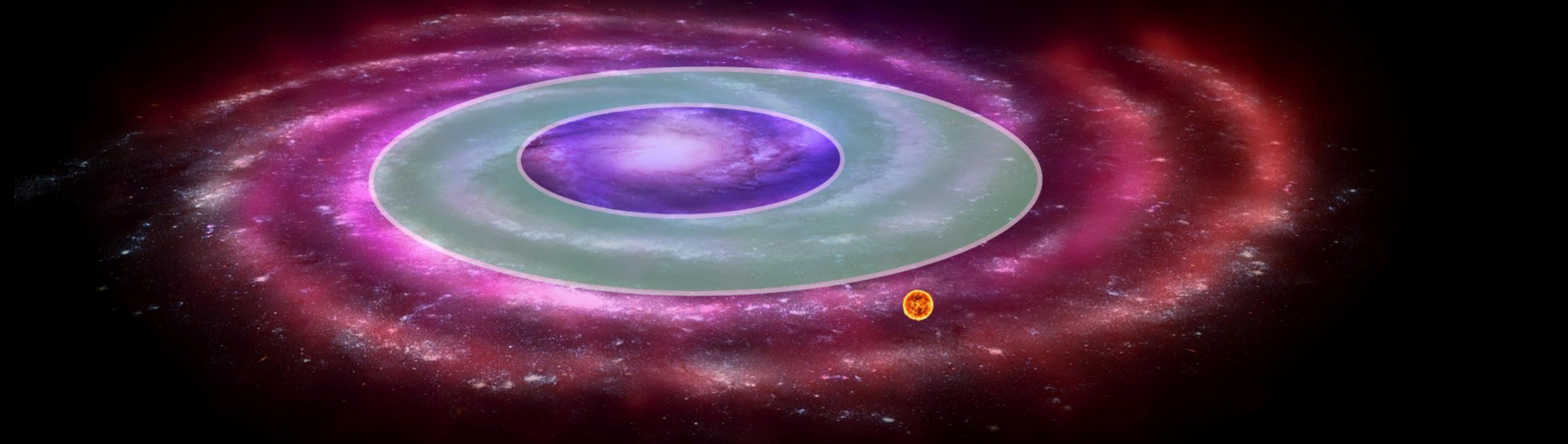
Modeling Strategy: gas maps divided in rings



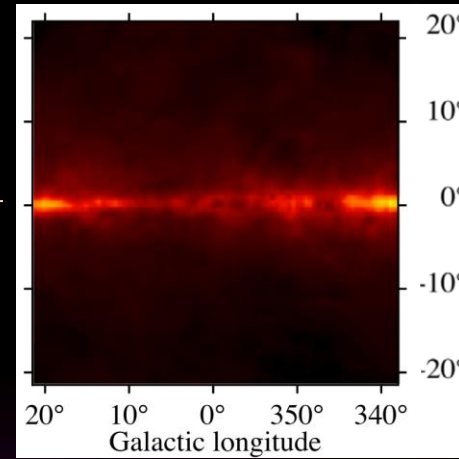
0 – 3.5 kpc,
Hydrogen gas



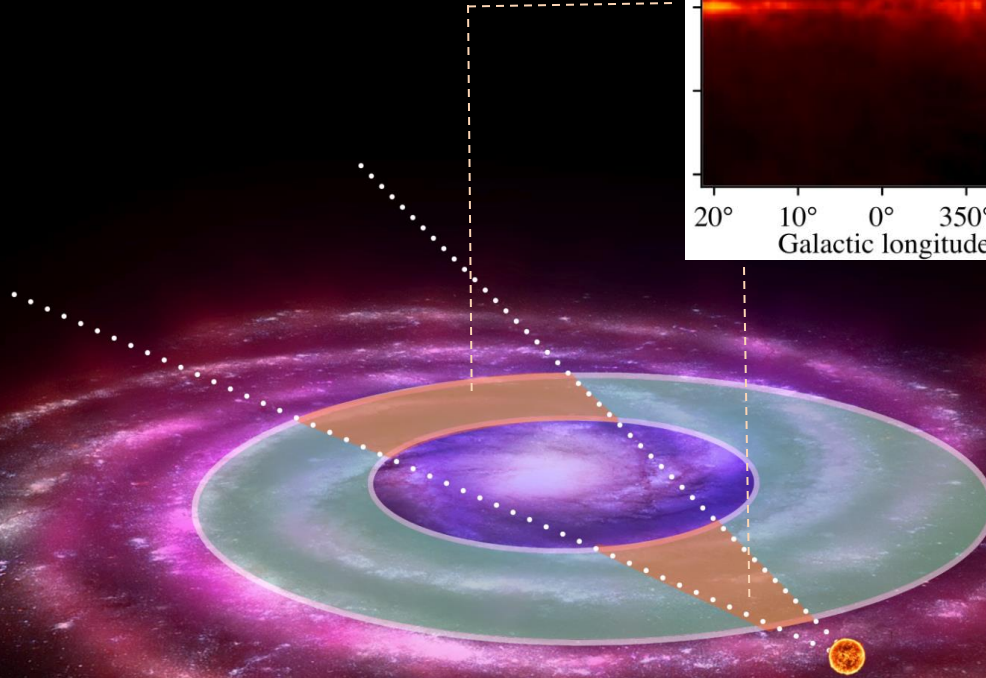
Modeling Strategy: gas maps divided in rings



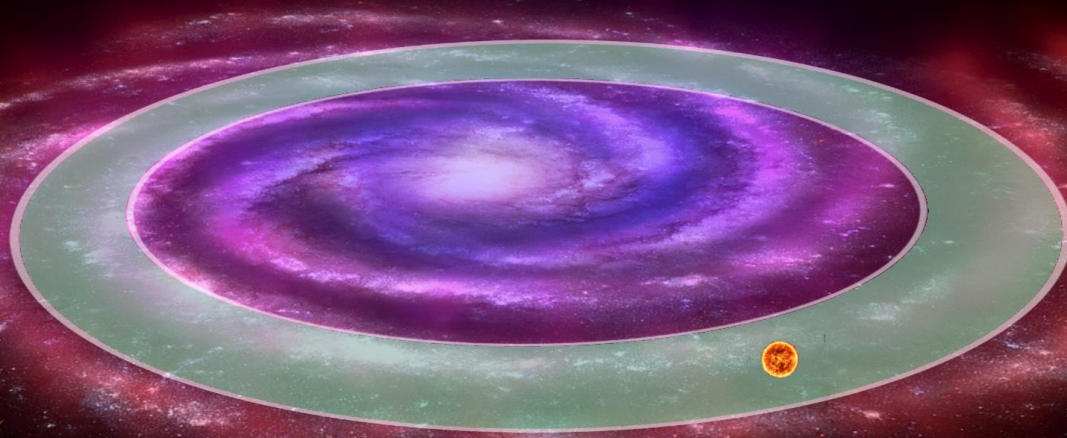
Modeling Strategy: gas maps divided in rings



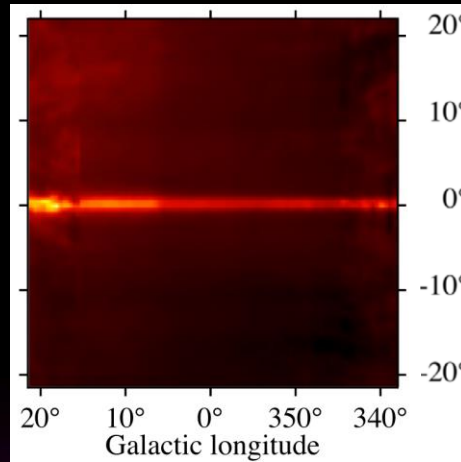
3.5 - 8.0 kpc,
Hydrogen gas



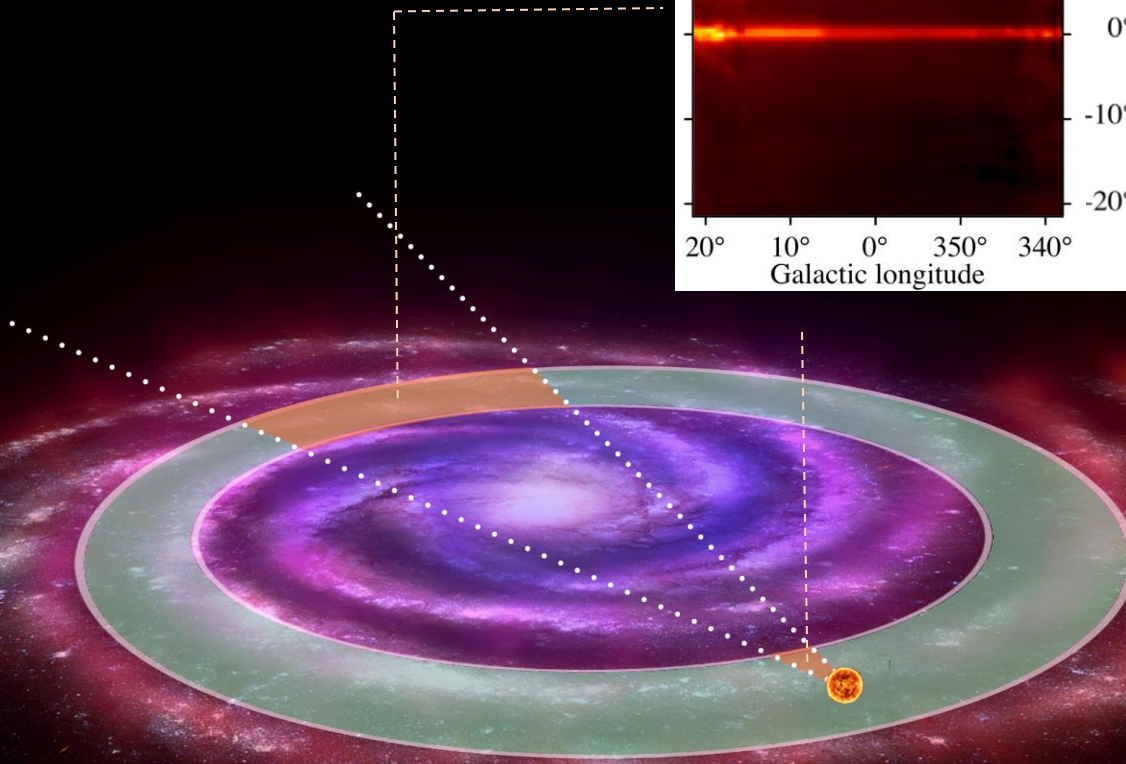
Modeling Strategy: gas maps divided in rings



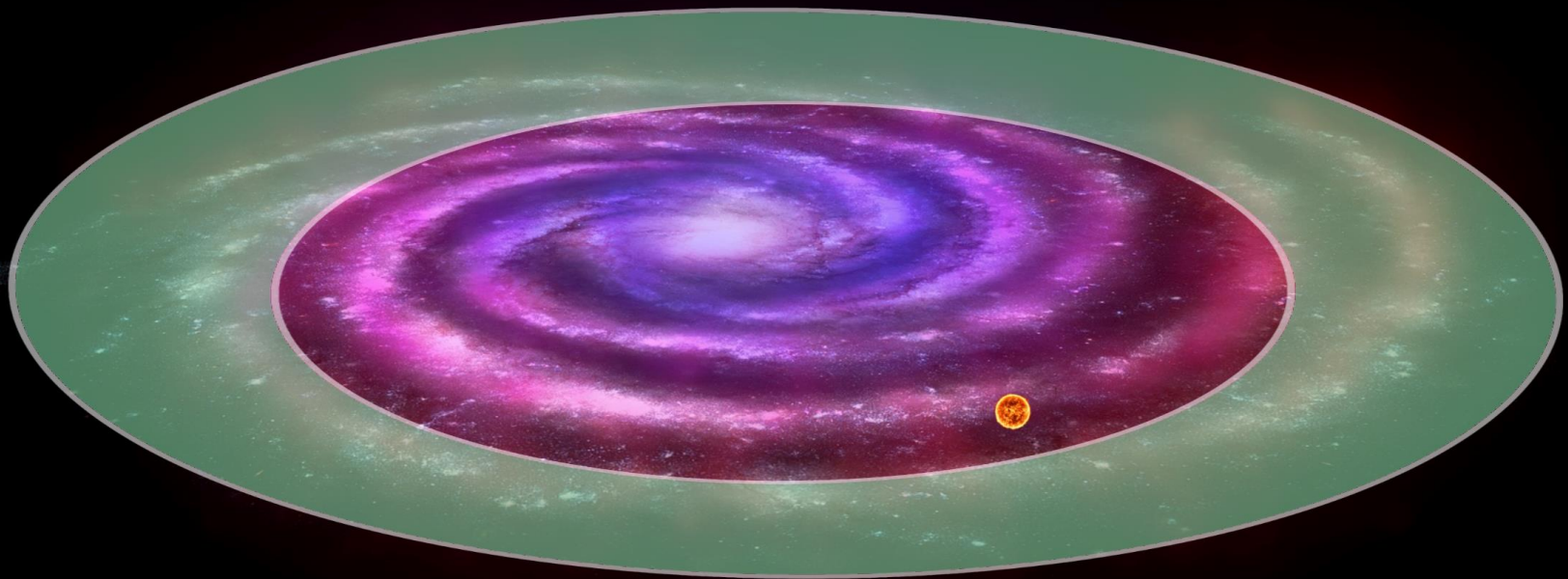
Modeling Strategy: gas maps divided in rings



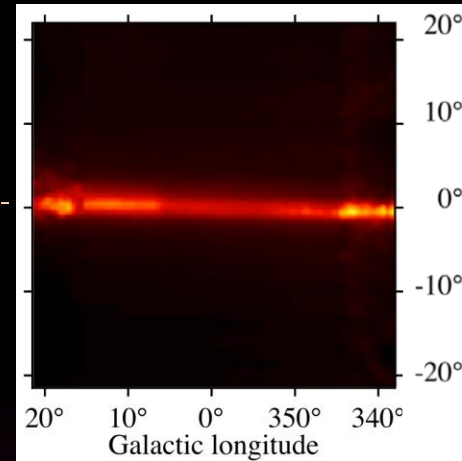
8 - 10 kpc,
Hydrogen gas



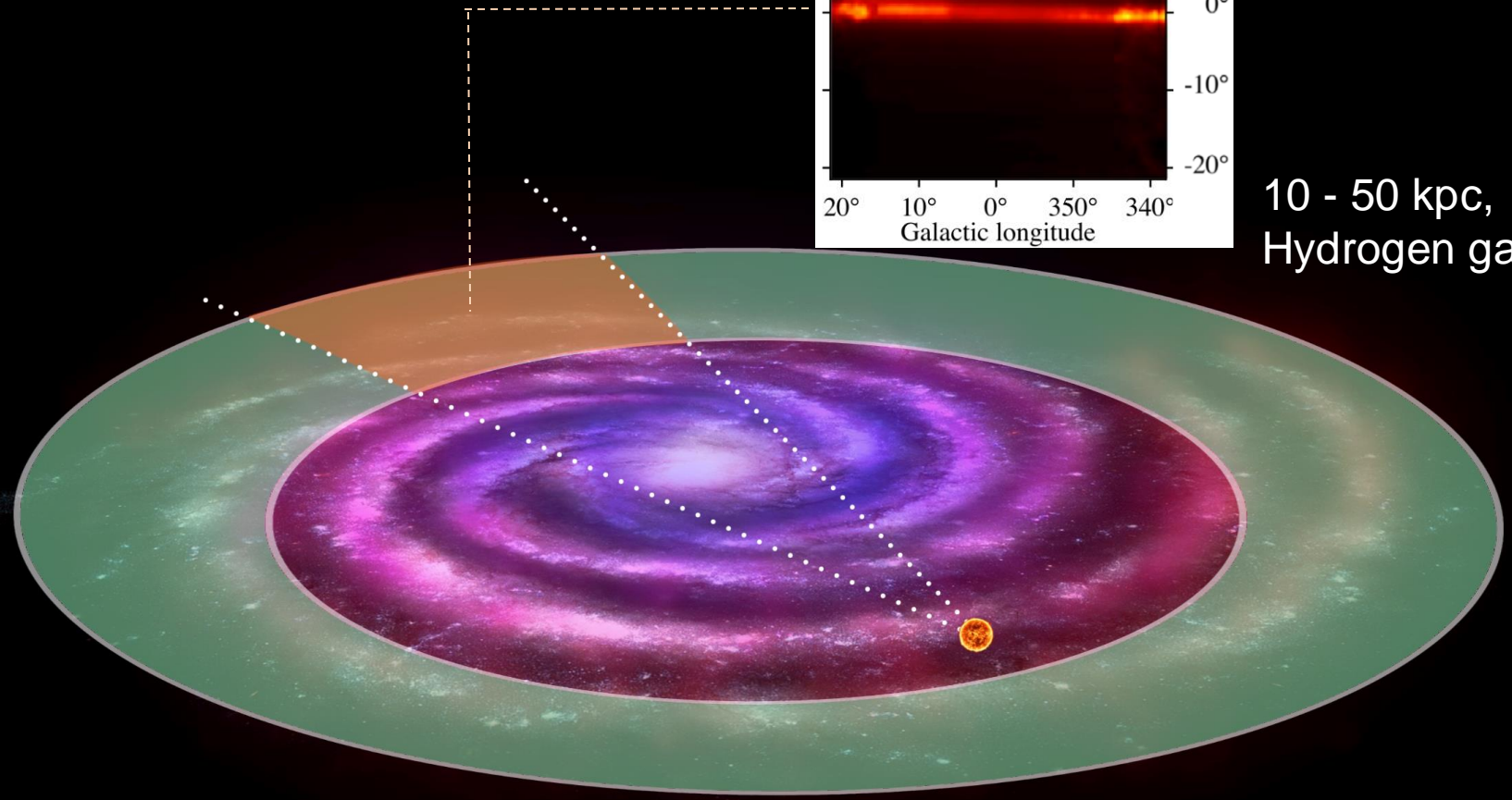
Modeling Strategy: gas maps divided in rings



Modeling Strategy: gas maps divided in rings

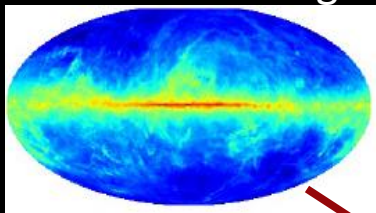


10 - 50 kpc,
Hydrogen gas

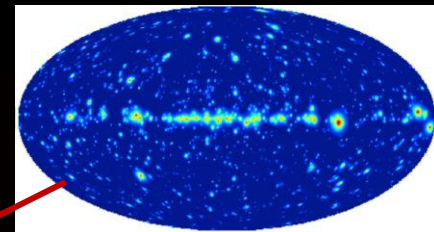


Modeling strategy: template fitting

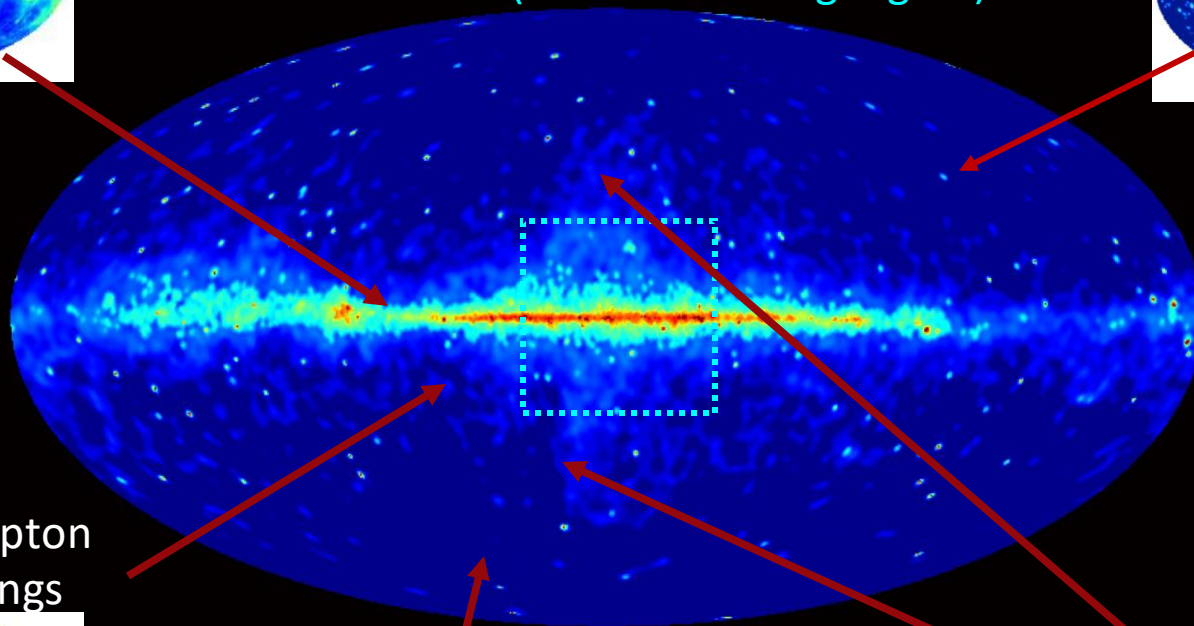
New hydrogen maps
divided in 4 rings



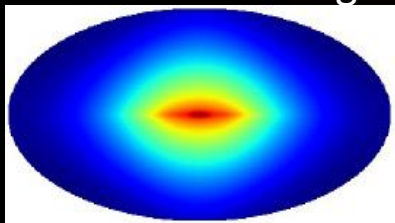
4FGL Catalog



Fermi-LAT data (inner 40x40 deg region)

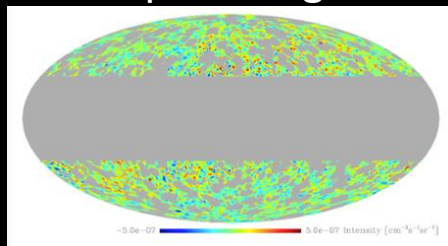


3D Inverse Compton
divided in 6 rings

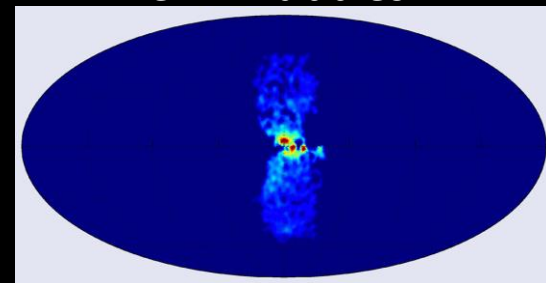


Porter et al. (2017)

Isotropic background

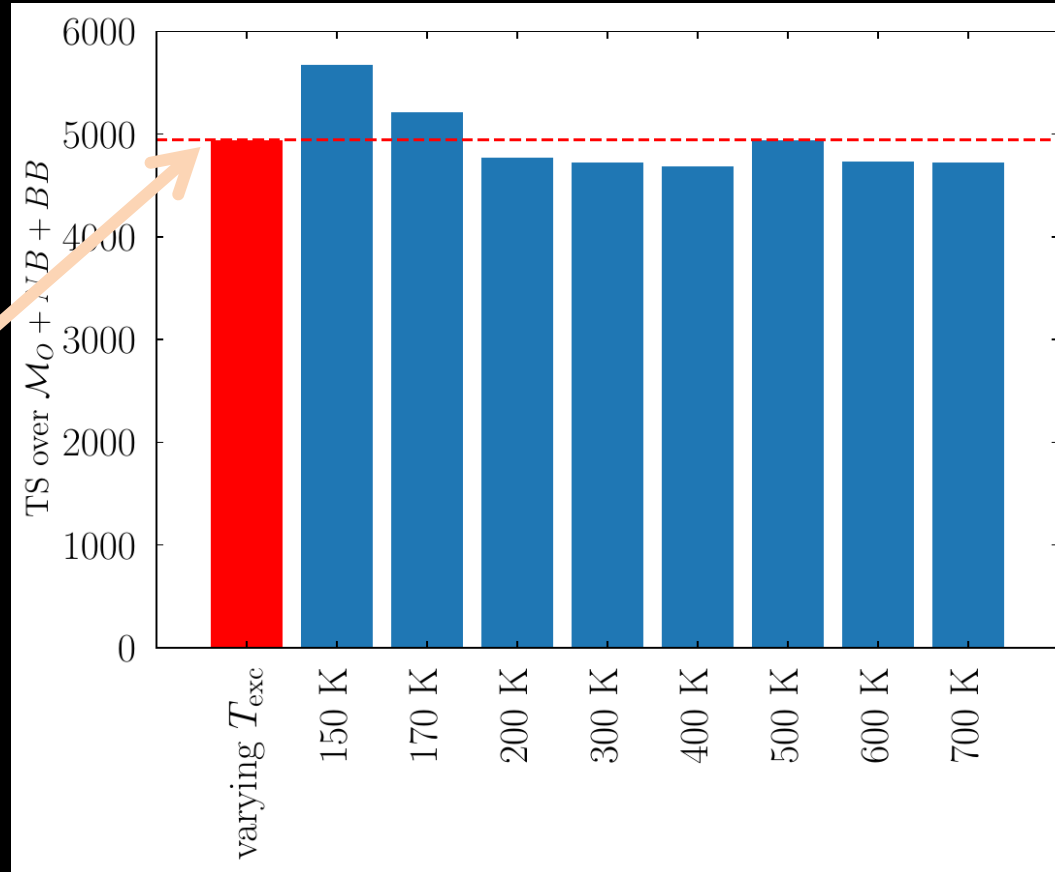


Fermi Bubbles



New background model much better

Significant improvement over our previous hydrodynamic maps



Test Statistic
over our old
background
model

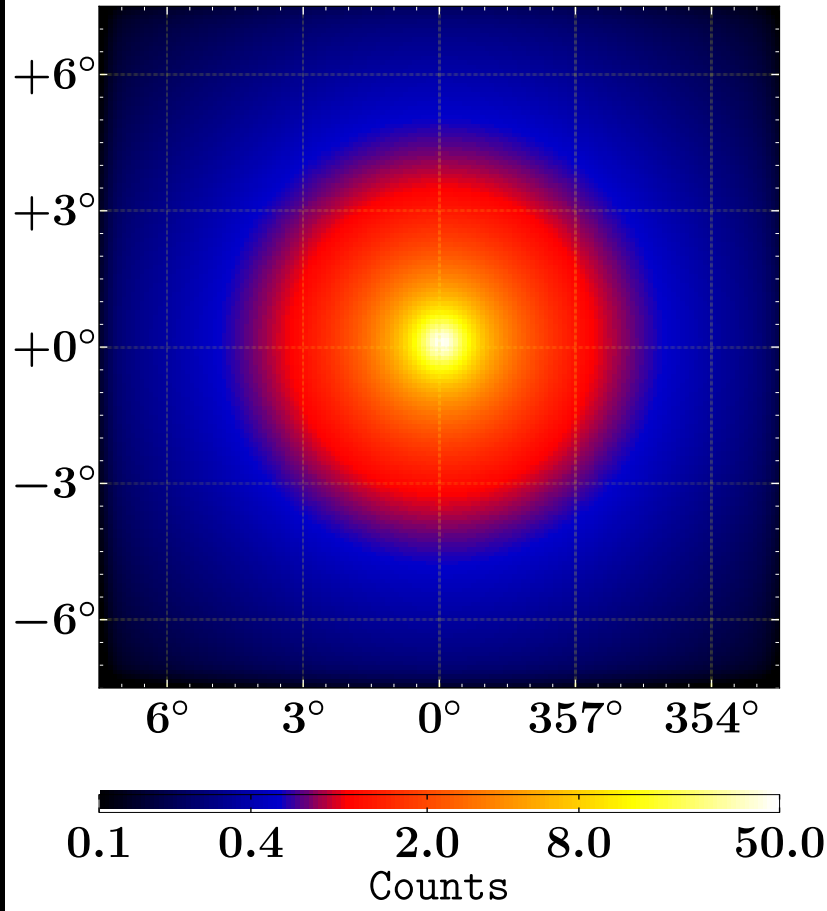
Pohl, OM, Coleman, Gordon (2022)

➔ New hydrogen maps are publicly available at <https://doi.org/10.5281/zenodo.6276721>

Spherical symmetry vs bulge shape

Navarro-Frenk-White profile

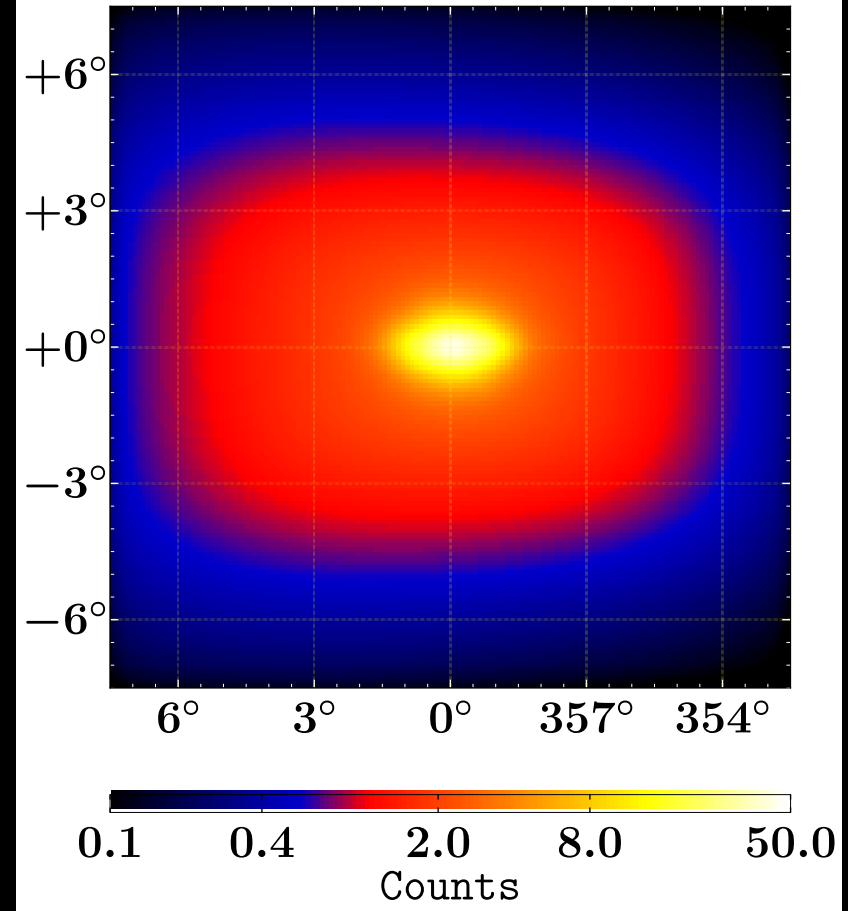
1.1 – 2.8 GeV



VS

Stellar Distribution

1.1 – 2.8 GeV



➔ We want to test which spatial template is preferred by the data

Statistical Results

Base model includes: new gas maps, 3D IC, Fermi bubbles, 4FGL sources, isotropic

Baseline Model	Additional Source	Δ TS	Significance
Base	Cored ellips.	0.0	0.0σ
Base	Cored	0.1	0.0σ
Base	BB	282.2	15.3σ
Base	NFW ellips.	647.2	24.2σ
Base	NFW	807.1	27.3σ
Base	NB	1728.9	40.8σ
Base+NB	Cored ellips.	0.1	0.0σ
Base+NB	Cored	0.7	0.0σ
Base+NB	NFW ellips.	1.0	0.0σ
Base+NB	NFW	3.4	0.2σ
Base+NB	BB	261.0	14.7σ
Base+NB+BB	NFW ellips.	0.1	0.0σ
Base+NB+BB	Cored ellips.	0.4	0.0σ
Base+NB+BB	Cored	0.7	0.0σ
Base+NB+BB	NFW	2.6	0.1σ

Pohl, OM, Coleman, Gordon (2022)

Statistical Results

Base model includes: new gas maps, 3D IC, Fermi bubbles, 4FGL sources, isotropic

Baseline Model	Additional Source	ΔTS	Significance
Base	Cored ellips.	0.0	0.0σ
Base	Cored	0.1	0.0σ
Base	BB	282.2	15.3σ
Base	NFW ellips.	647.2	24.2σ
Base	NFW	807.1	27.3σ
Base	NB	1728.9	40.8σ
Base+NB	Cored ellips.	0.1	0.0σ
Base+NB	Cored	0.7	0.0σ
Base+NB	NFW ellips.	1.0	0.0σ
Base+NB	NFW	3.4	0.2σ
Base+NB	BB	261.0	14.7σ
Base+NB+BB	NFW ellips.	0.1	0.0σ
Base+NB+BB	Cored ellips.	0.4	0.0σ
Base+NB+BB	Cored	0.7	0.0σ
Base+NB+BB	NFW	2.6	0.1σ

Pohl, OM, Coleman, Gordon (2022)

Statistical Results

Base model includes: new gas maps, 3D IC, Fermi bubbles, 4FGL sources, isotropic

Baseline Model	Additional Source	ΔTS	Significance
Base	Cored ellips.	0.0	0.0σ
Base	Cored	0.1	0.0σ
Base	BB	282.2	15.3σ
Base	NFW ellips.	647.2	24.2σ
Base	NFW	807.1	27.3σ
Base	NB	1728.9	40.8σ
Base+NB	Cored ellips.	0.1	0.0σ
Base+NB	Cored	0.7	0.0σ
Base+NB	NFW ellips.	1.0	0.0σ
Base+NB	NFW	3.4	0.2σ
Base+NB	BB	261.0	14.7σ
Base+NB+BB	NFW ellips.	0.1	0.0σ
Base+NB+BB	Cored ellips.	0.4	0.0σ
Base+NB+BB	Cored	0.7	0.0σ
Base+NB+BB	NFW	2.6	0.1σ

Pohl, OM, Coleman, Gordon (2022)

Statistical Results

Base model includes: new gas maps, 3D IC, Fermi bubbles, 4FGL sources, isotropic

Baseline Model	Additional Source	Δ TS	Significance
Base	Cored ellips.	0.0	0.0σ
Base	Cored	0.1	0.0σ
Base	BB	282.2	15.3σ
Base	NFW ellips.	647.2	24.2σ
Base	NFW	807.1	27.3σ
Base	NB	1728.9	40.8σ
Base+NB	Cored ellips.	0.1	0.0σ
Base+NB	Cored	0.7	0.0σ
Base+NB	NFW ellips.	1.0	0.0σ
Base+NB	NFW	3.4	0.2σ
Base+NB	BB	261.0	14.7σ
Base+NB+BB	NFW ellips.	0.1	0.0σ
Base+NB+BB	Cored ellips.	0.4	0.0σ
Base+NB+BB	Cored	0.7	0.0σ
Base+NB+BB	NFW	2.6	0.1σ

Pohl, OM, Coleman, Gordon (2022)

Statistical Results

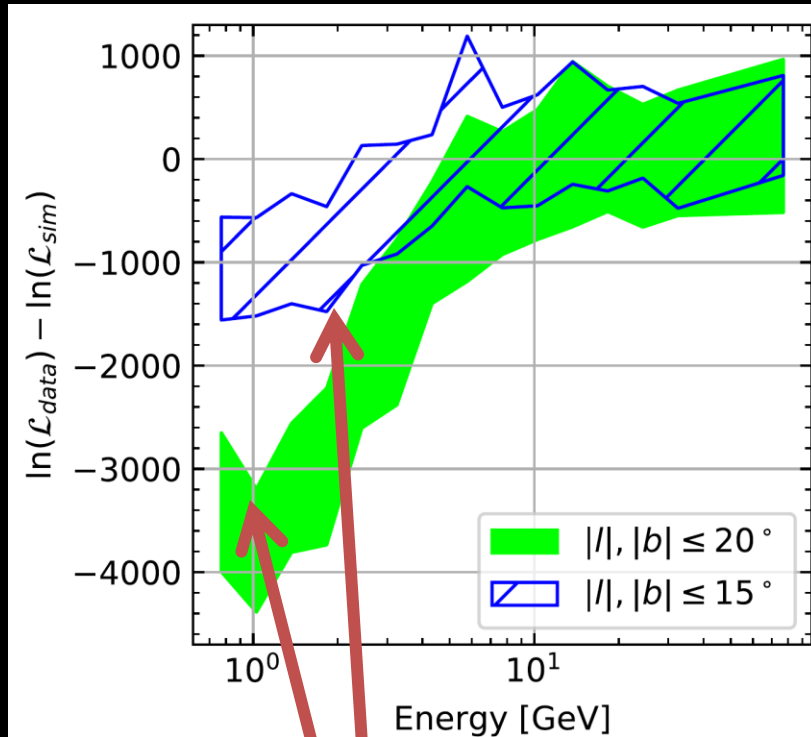
Base model includes: new gas maps, 3D IC, Fermi bubbles, 4FGL sources, isotropic

Baseline Model	Additional Source	Δ TS	Significance
Base	Cored ellips.	0.0	0.0σ
Base	Cored	0.1	0.0σ
Base	BB	282.2	15.3σ
Base	NFW ellips.	647.2	24.2σ
Base	NFW	807.1	27.3σ
Base	NB	1728.9	40.8σ
Base+NB	Cored ellips.	0.1	0.0σ
Base+NB	Cored	0.7	0.0σ
Base+NB	NFW ellips.	1.0	0.0σ
Base+NB	NFW	3.4	0.2σ
Base+NB	BB	261.0	14.7σ
Base+NB+BB	NFW ellips.	0.1	0.0σ
Base+NB+BB	Cored ellips.	0.4	0.0σ
Base+NB+BB	Cored	0.7	0.0σ
Base+NB+BB	NFW	2.6	0.1σ

See also Macias et al. Nat. Astr. (2018) and Bartels et al. Nat. Astr. (2018)

Goodness of the fit

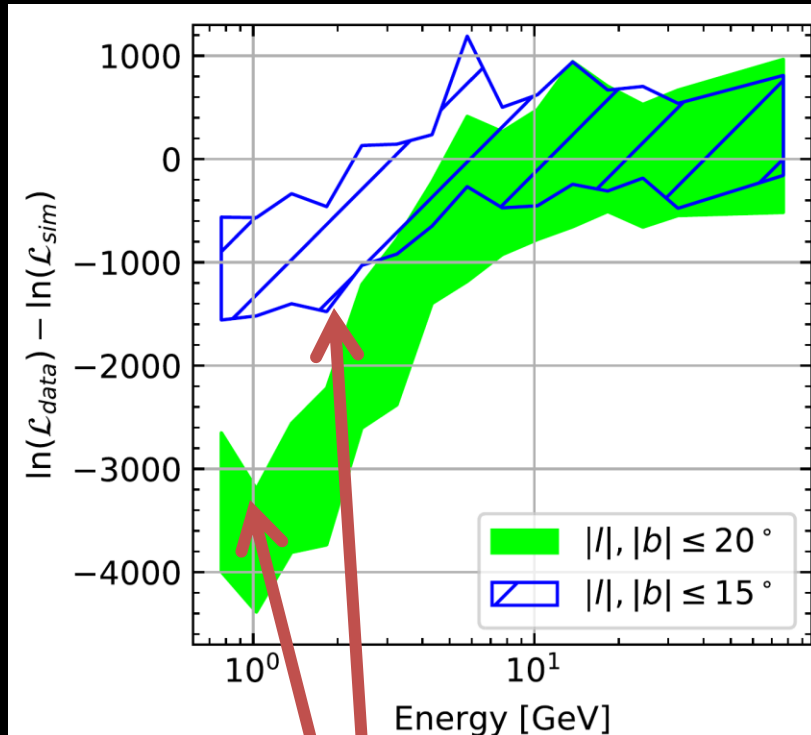
Pohl, OM, Coleman, Gordon (2022)



**Comparisons with Monte Carlo
Expectations (point sources fitted)**

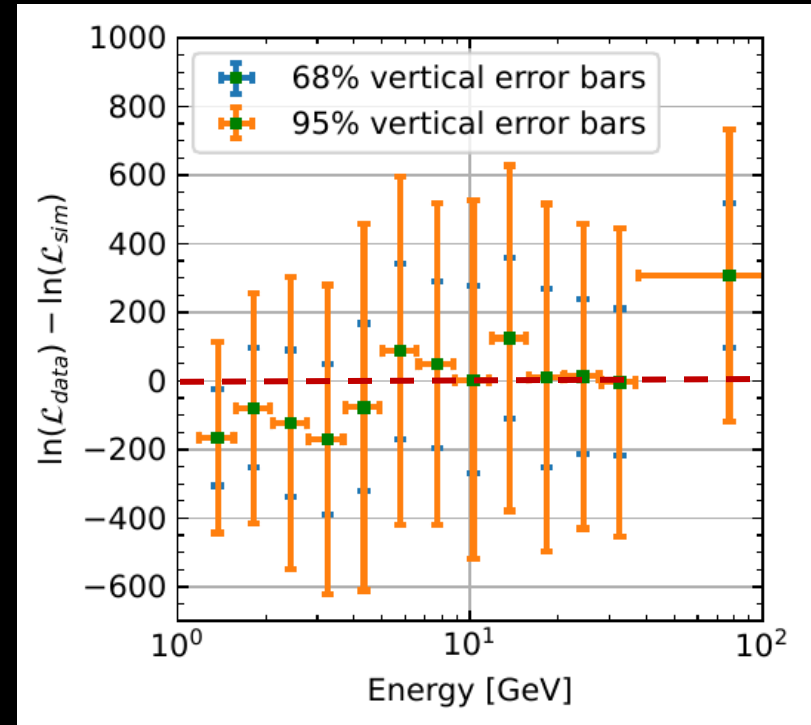
Goodness of the fit

Pohl, OM, Coleman, Gordon (2022)



Comparisons with Monte Carlo Expectations (point sources fitted)

Gordon, OM, Pohl (In preparation)



Log-likelihood results agree with MC expectations when point sources are masked

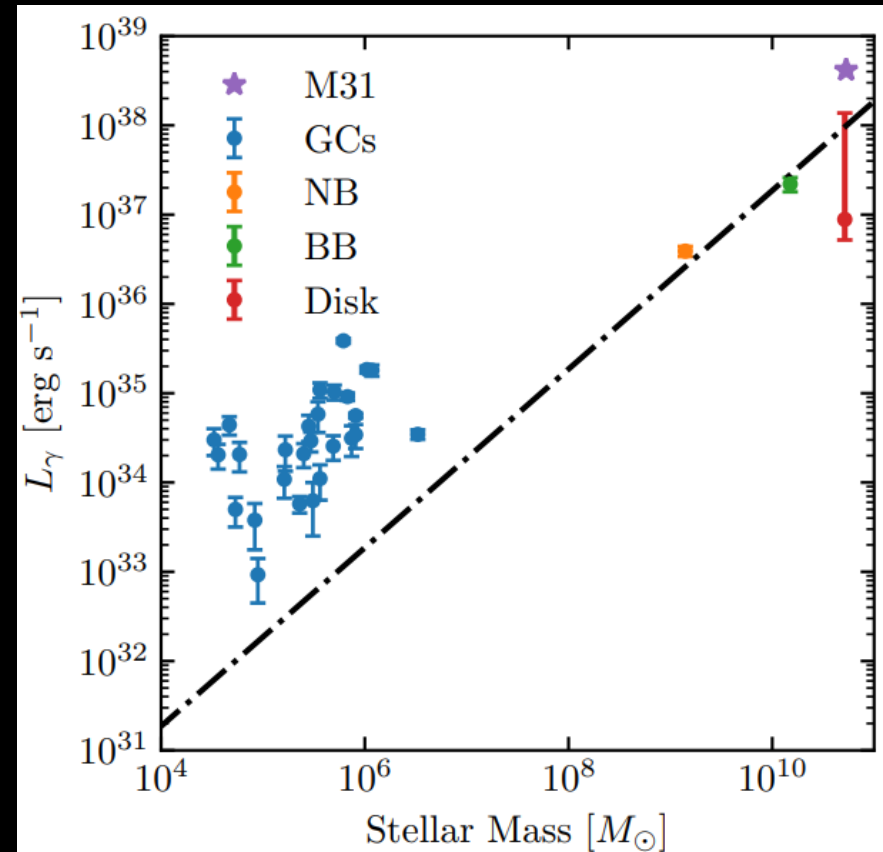
Comparison of regions

Gamma ray to mass ratios

Shows environmental dependence of MSP gamma rays

- Boxy bulge, nuclear bulge, Milky Way disk (from MSPs) consistent with each other
- Globular clusters higher by factor ~ 10 -40, explained by large dynamical channel
- M31 also higher, consistent with its higher encounter rate.

Song, OM, Horiuchi, Crocker, Nataf (2021)



See also Bartels et al (2018), Eckner et al (2018)

Conclusions

We have released new hydrogen gas maps which account for continuum emission and absorption.

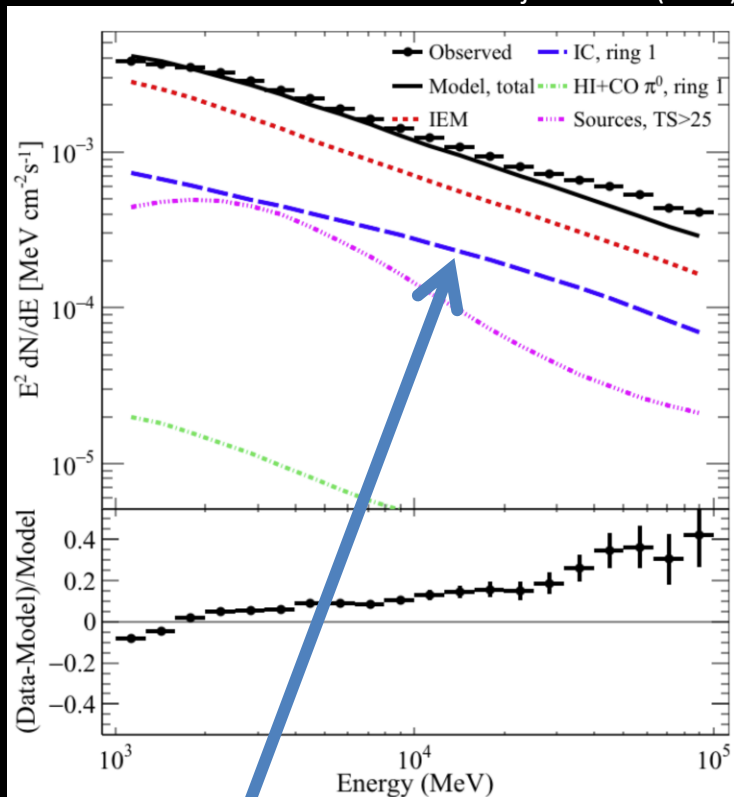
The new gas maps provide a much better fit to Fermi-LAT observations of the Galactic center.

We confirm previous results that the stellar bulge hypothesis is preferred to the dark matter explanation for the GCE.

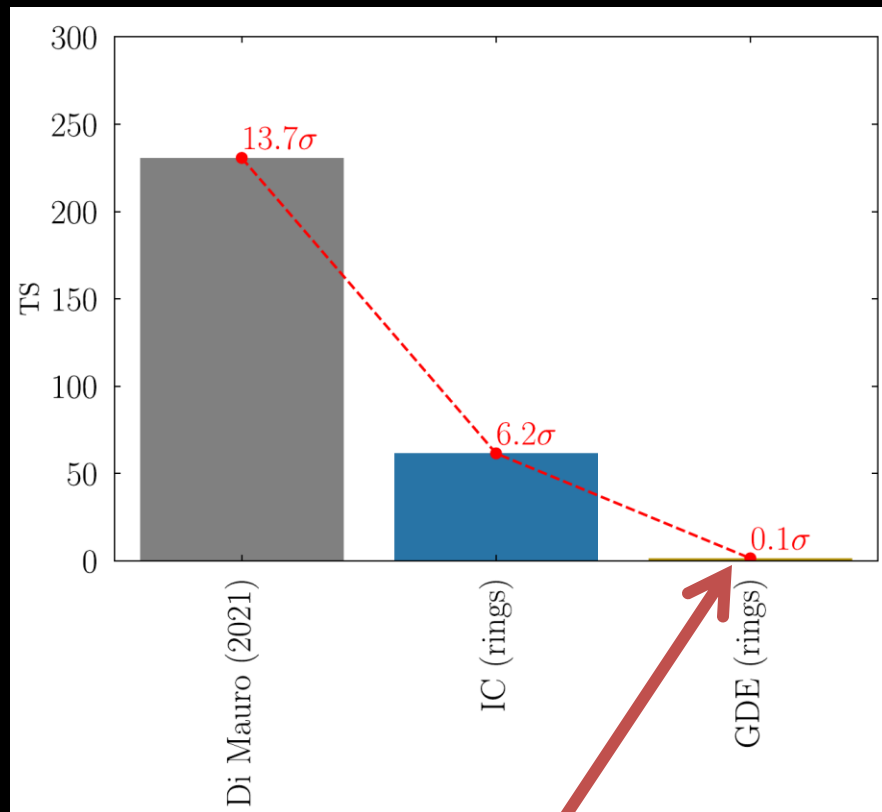
BACK-UP SLIDES

Flexibility of the Galactic diffuse emission

Ajello et al. (2015)



Pohl, OM, Coleman, Gordon (2022)



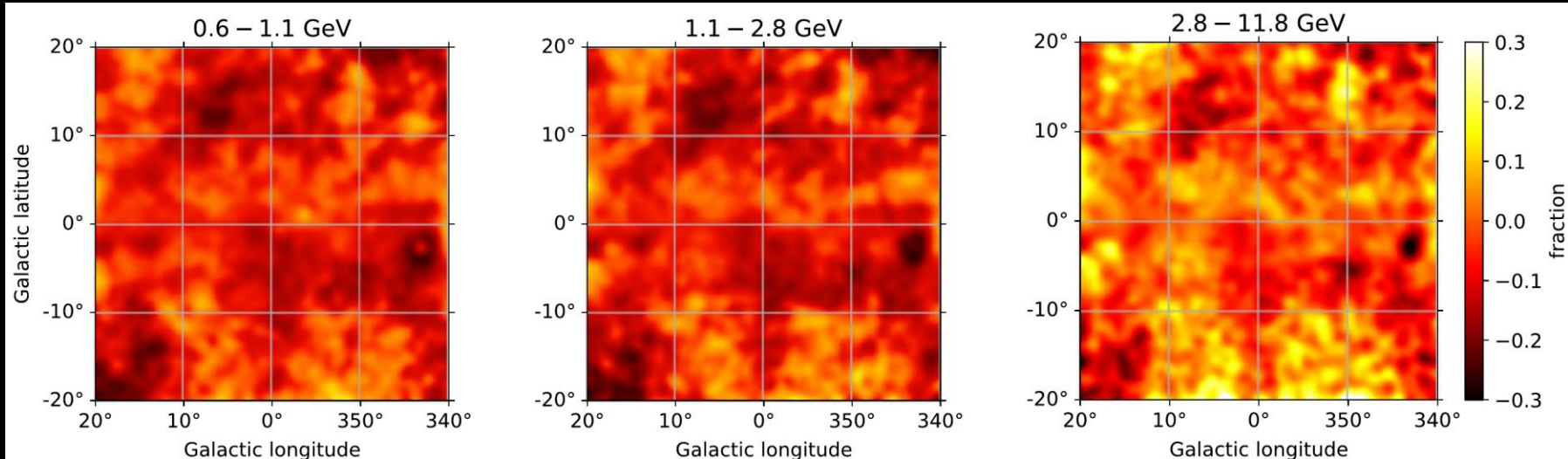
Enhanced IC emission in the inner Galaxy

The evidence for dark matter goes away when the GDE models are divided in rings

Residual Images

Residuals are small, except in a few localized regions

Pohl, OM, Coleman, Gordon (2022)



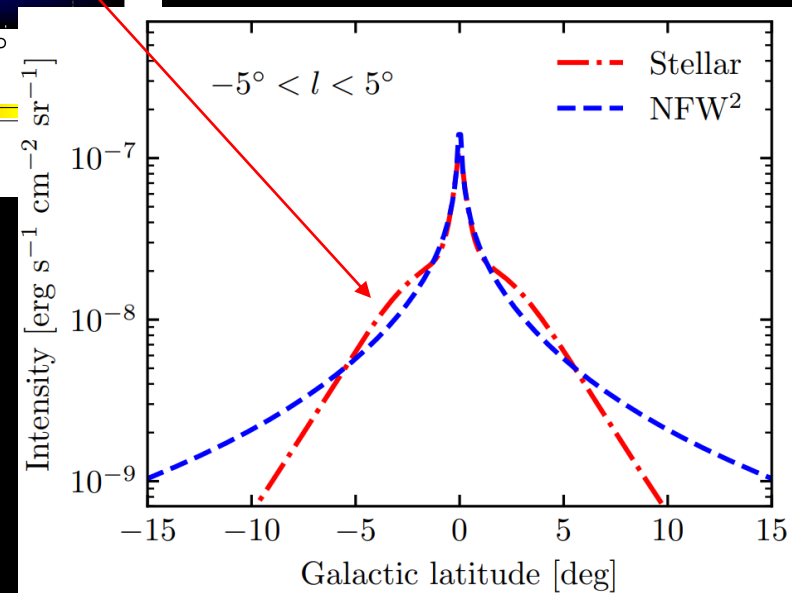
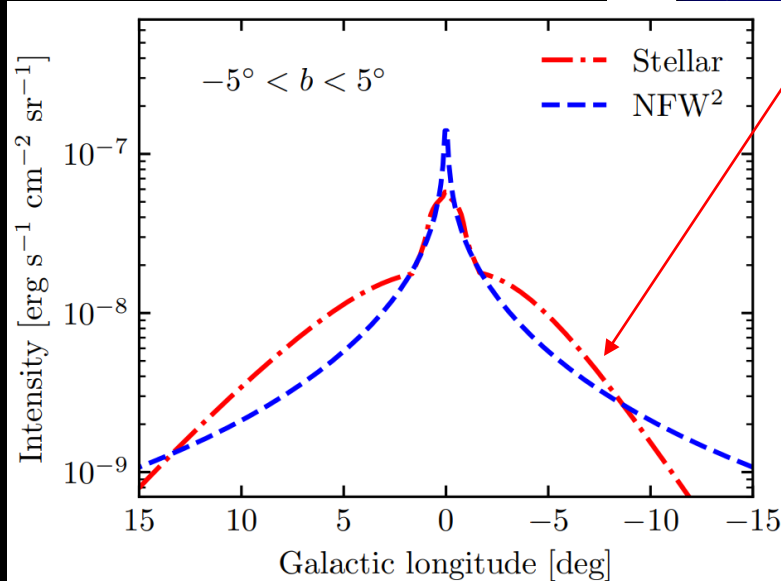
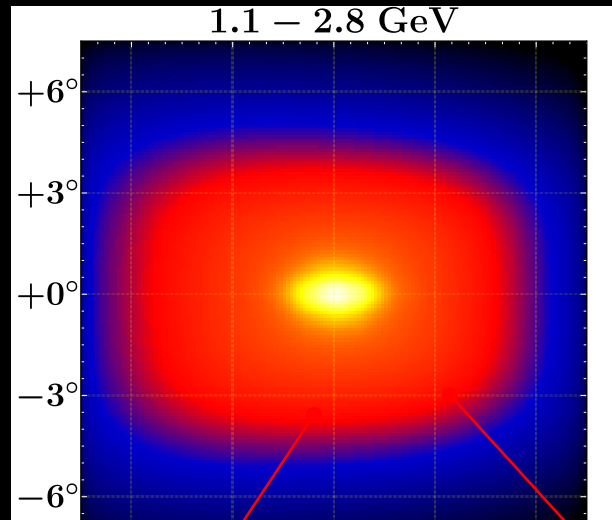
Some correlated residuals remain, possibly due to mismodeling of point sources and/or the Fermi bubbles.

How are the two distinguished?

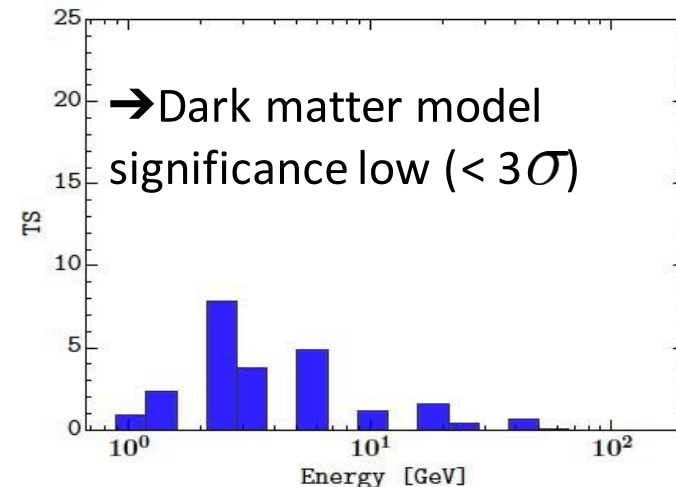
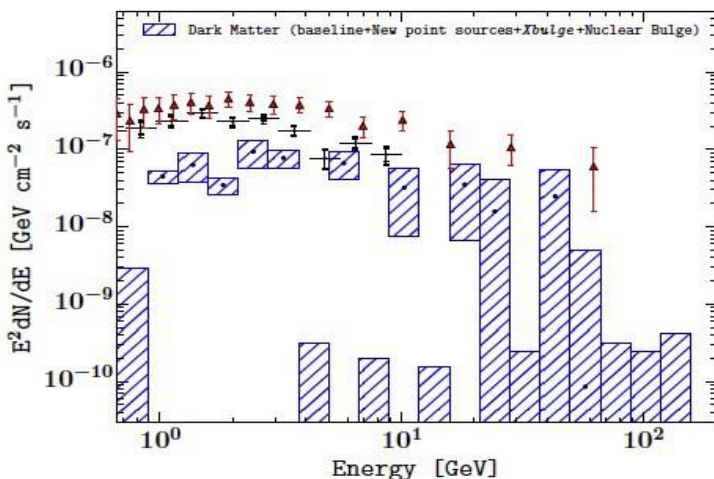
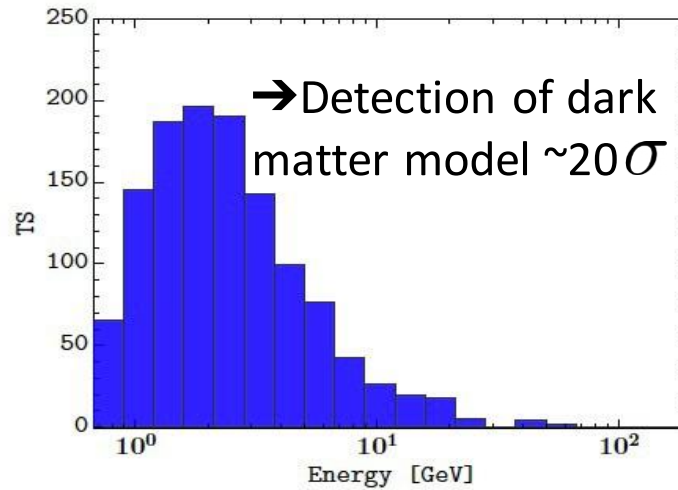
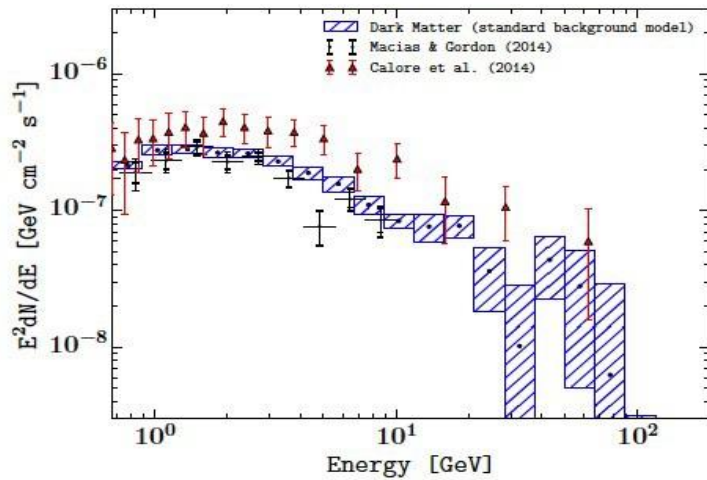
Q: why didn't previous dark matter model deformation studies discover a deviation from sphericity?

A: Tilted bar seen from the side has unique radius-dependent longitudinal shape

Song, OM, Horiuchi (2019)



Galactic bulge preferred over dark matter for the Galactic centre gamma-ray excess



Macias+(2018)

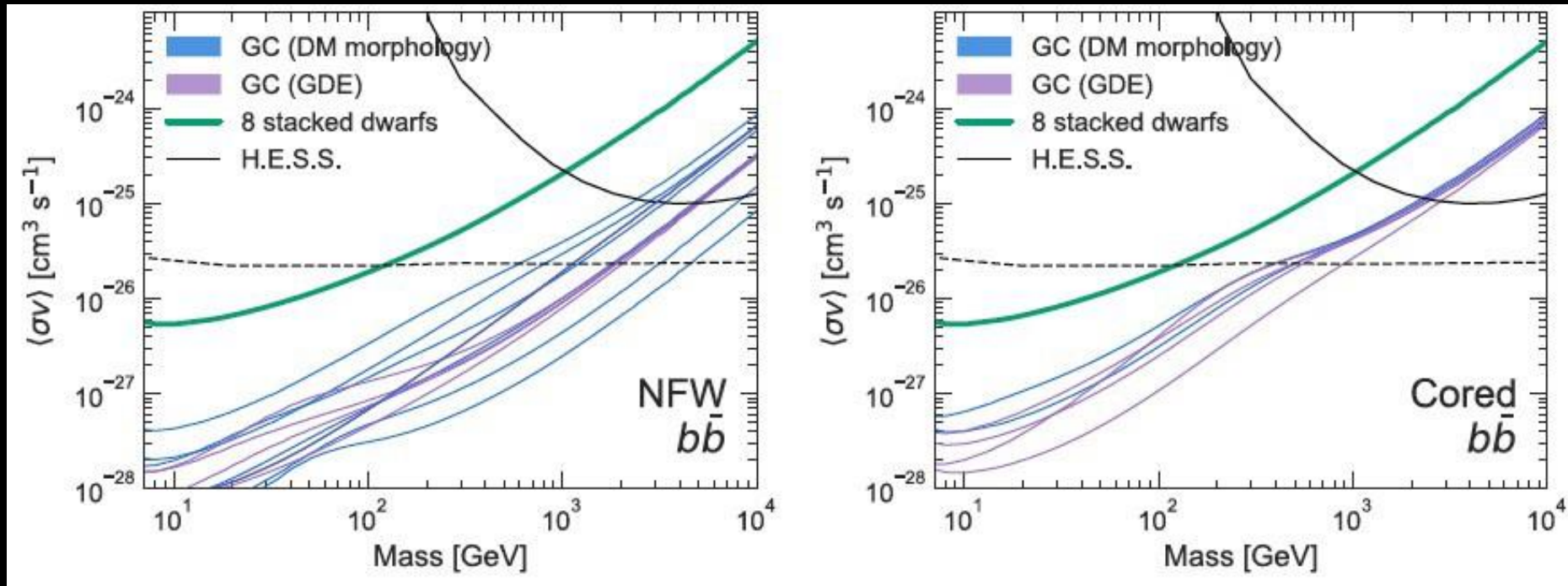
↙ **WITHOUT bulge**
(representative of previous studies)

↙ **WITH bulge**
Including our bulge model the data no longer needs a dark matter component

Improved sensitivity to dark matter

We addressed a major systematic, which allowed us to realize the potential of the Galactic Center to constrain dark matter

Abazajian, Horiuchi, Kaplinghat, Keeley, OM (2020)



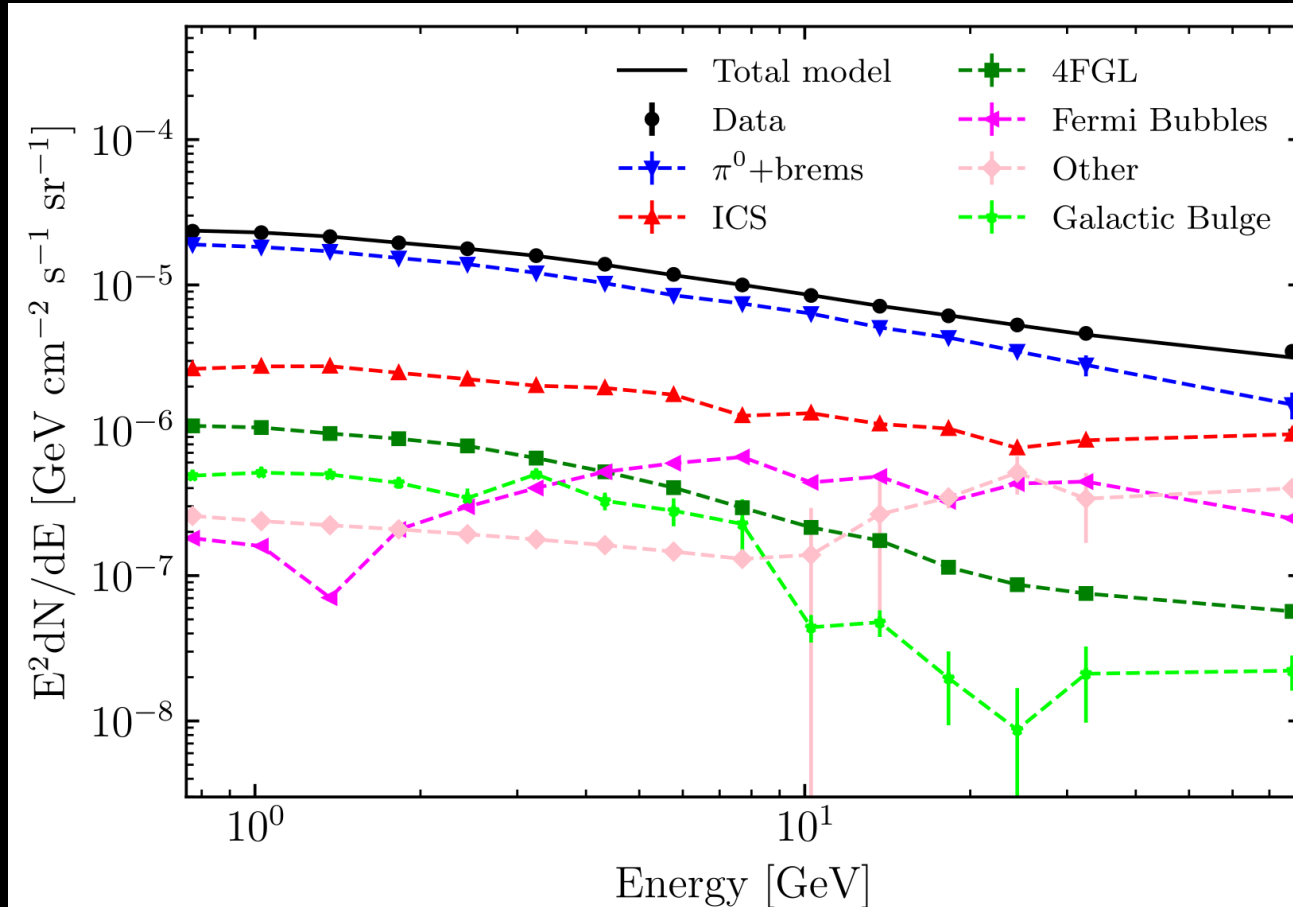
- Impacts of NFW slope [0.5,1.5] & sphericity
- Impacts of background modeling

- Impacts of core (1 kpc) & sphericity
- Impacts of background modeling

→ Tests thermal dark matter out to ~500 GeV

Spectrum of the Fermi GeV excess

Pohl, OM, Coleman, Gordon (2022)



➔ Spectrum of the stellar bulge template

Checks for systematics

Gas maps: using the gas maps used by the Fermi Diffuse models yield the same conclusions
Macias et al. (2018)

Base	Source	$\log(\mathcal{L}_{\text{Base}})$	$\log(\mathcal{L}_{\text{Base+Source}})$	$\text{TS}_{\text{Source}}$	σ	Number of source parameters
baseline-NB+Boxy	NFW	-172005.9	-171999.0	13.8	1.4	19
baseline+NFW	NB+Boxy	-172167.9	-171999.0	337.8	18.3	2×19
baseline*	NFW	-173565.0	-172929.2	1272	34.6	19
baseline*+NFW	NB+Boxy	-172929.2	-172533.0	792.4	28.2	2×19
baseline*+NB+Boxy	NFW	-172547.4	-172533.0	28.8	3.0	19

Point sources: using none or the 2FIG point source catalog yield the same conclusions

baseline	2FIG	-172461.4	-170710.5	3501	37.3	81×19
baseline+2FIG	Boxy	-170710.5	-170536.3	348.4	18.7	19
baseline+2FIG	NFW	-170710.5	-170484.6	452	19.9	19
baseline+2FIG	NB	-170710.5	-170470.5	480	20.6	19
baseline+2FIG+NB	NFW	-170470.5	-170387.8	165	11.1	19
baseline+2FIG+NB	Boxy	-170470.5	-170317.2	306.6	17.5	19
baseline-2FIG+NB+Boxy	NFW	-170317.2	-170313.5	7.4	0.5	19

Galactic plane mask: using a $|b| < 1$ deg mask yields the same conclusions

baseline	NFW	-430824.6	-430696.9	255	14.4	19
baseline	Boxy	-430824.6	-430626.1	397	18.5	19
baseline	NP	-430824.6	-430189.9	1269	35.6	22×19
baseline+NP	NFW	-430189.9	-430097.0	186	12.0	19
baseline+NP	Boxy	-430189.9	-430035.8	308	16.1	19
baseline+NP+Boxy	NFW	-430035.8	-430026.3	19	2.0	19

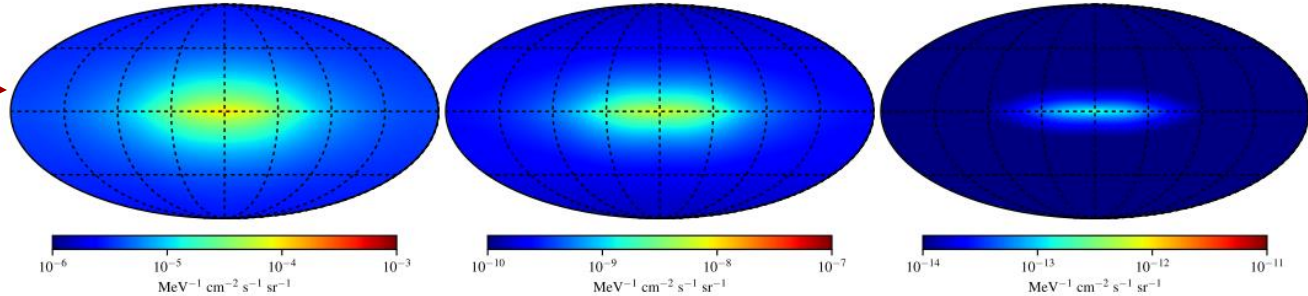
New 3D Inverse Compton Maps

10.6 MeV

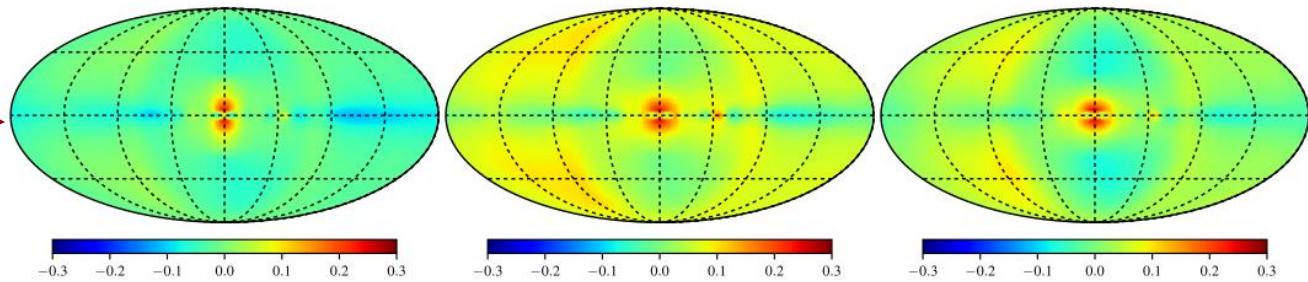
1.2 GeV

79 GeV

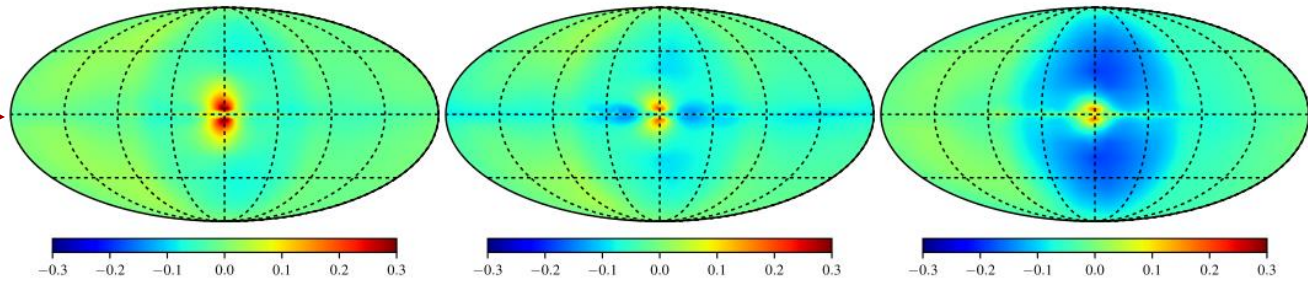
Standard 2D IC



New 3D IC:
Fractional residual for
R12 Model



New 3D IC:
Fractional residual for
F98 Model

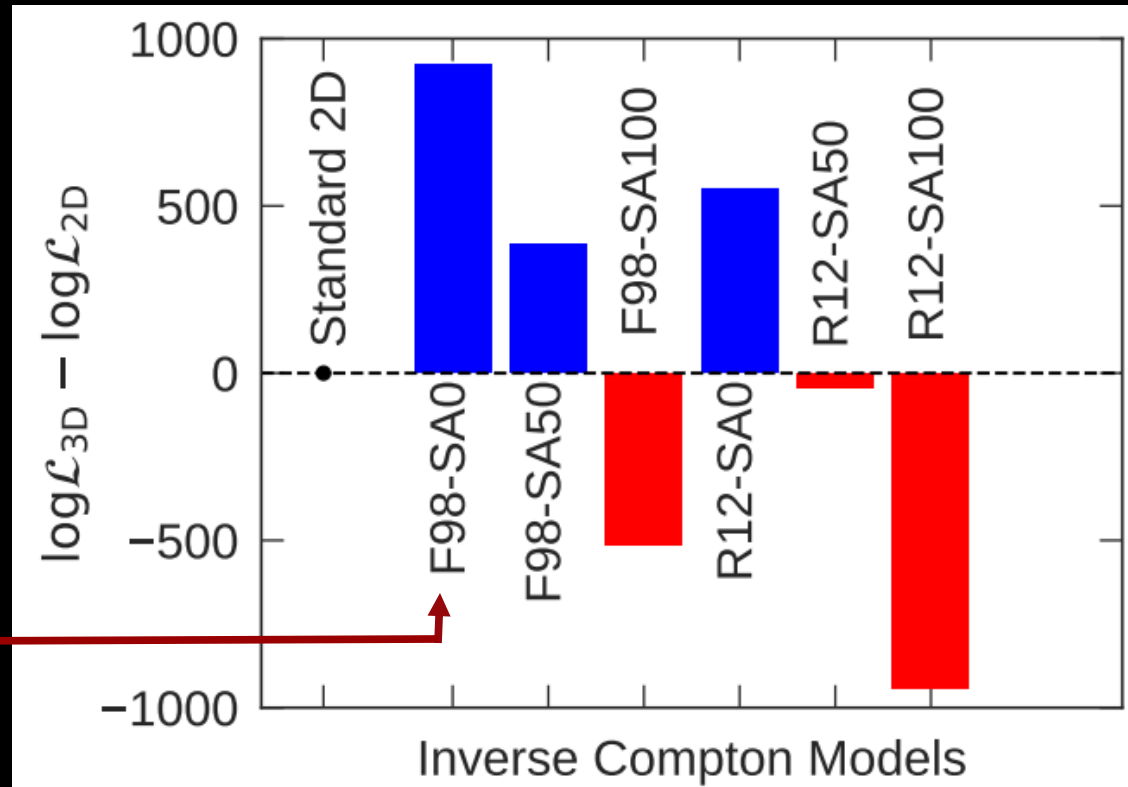
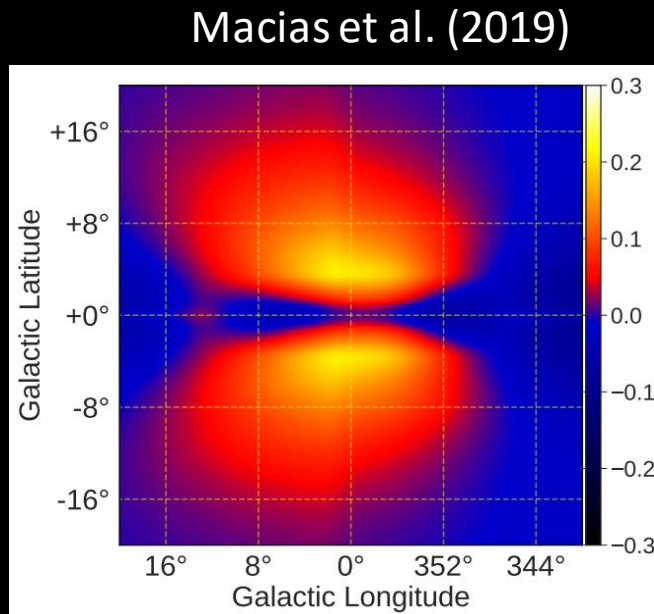


Porter et al. ApJ. (2017)

New 3D Inverse Compton maps

The data highly prefers the new 3D IC map *F98-SA0* over the Standard 2D IC map.

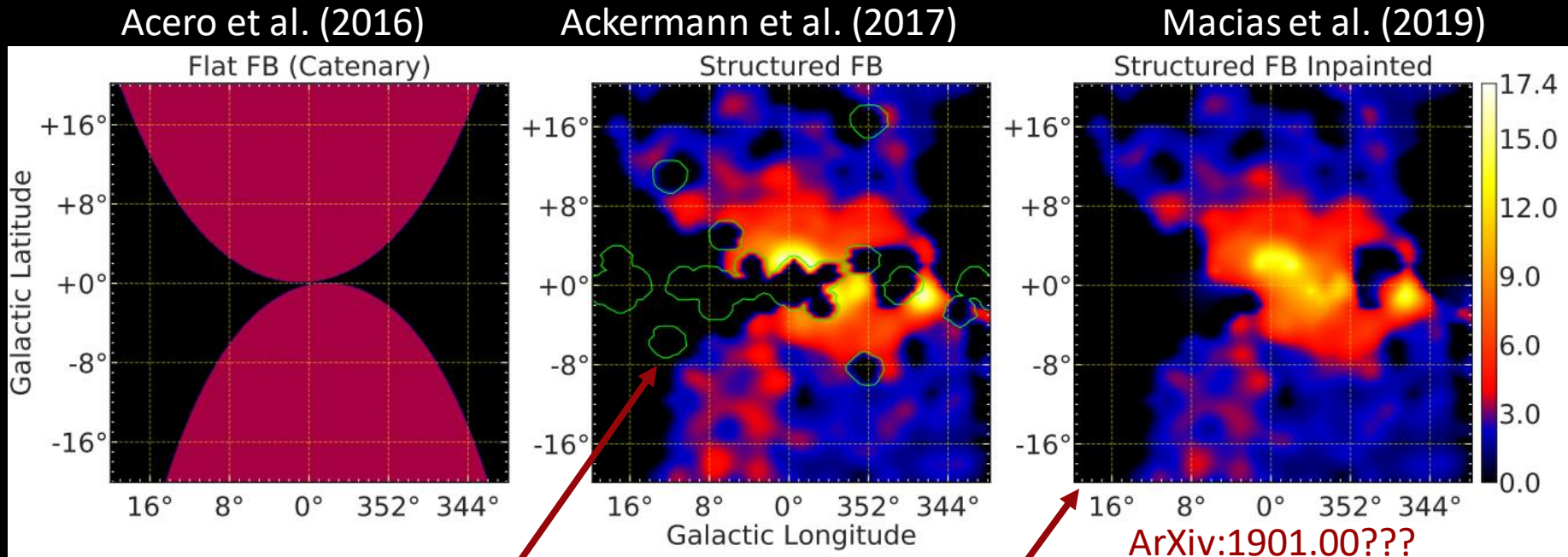
Macias et al. JCAP (2019)



Fractional residual for **F98** Model in the Galactic Center

Low-latitude Fermi Bubbles map

Used an inpainting method to correct artifacts in available maps



Artifacts due to point source mask

Correction after inpainting method

Low-latitude Fermi Bubbles map

Inpainted Fermi bubbles map significantly improves the fit

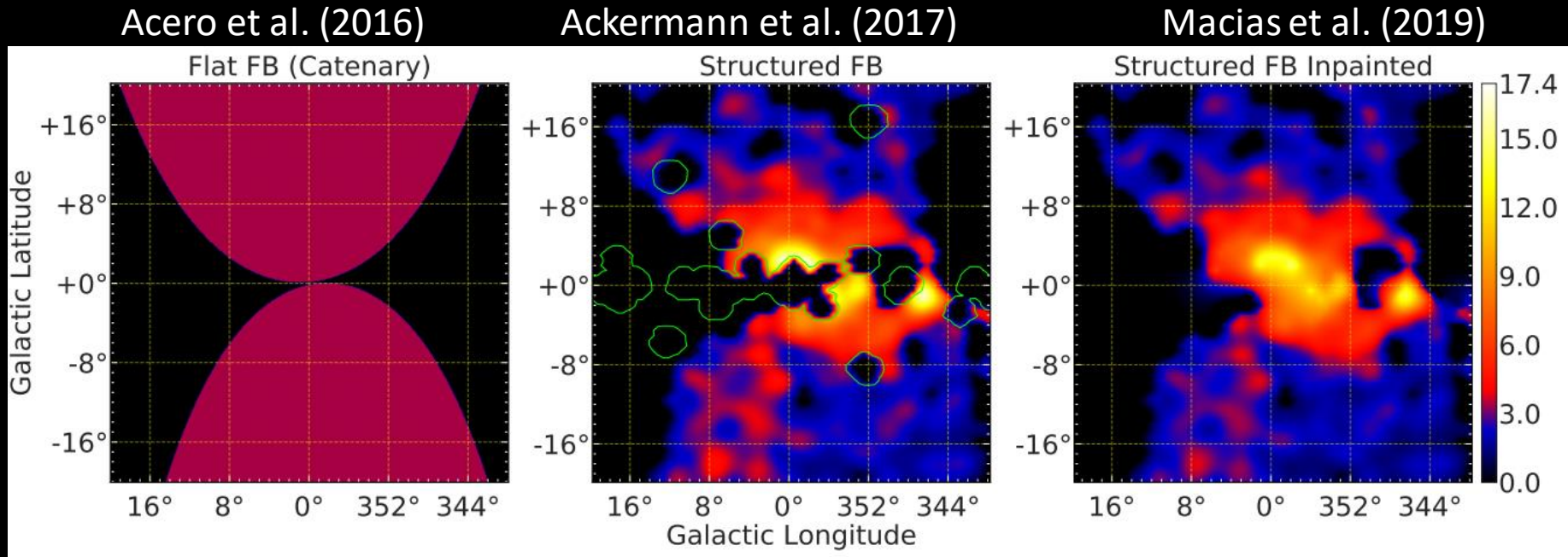


TABLE II. Summary of the likelihood analyses for 3 alternative *Fermi* bubbles maps.

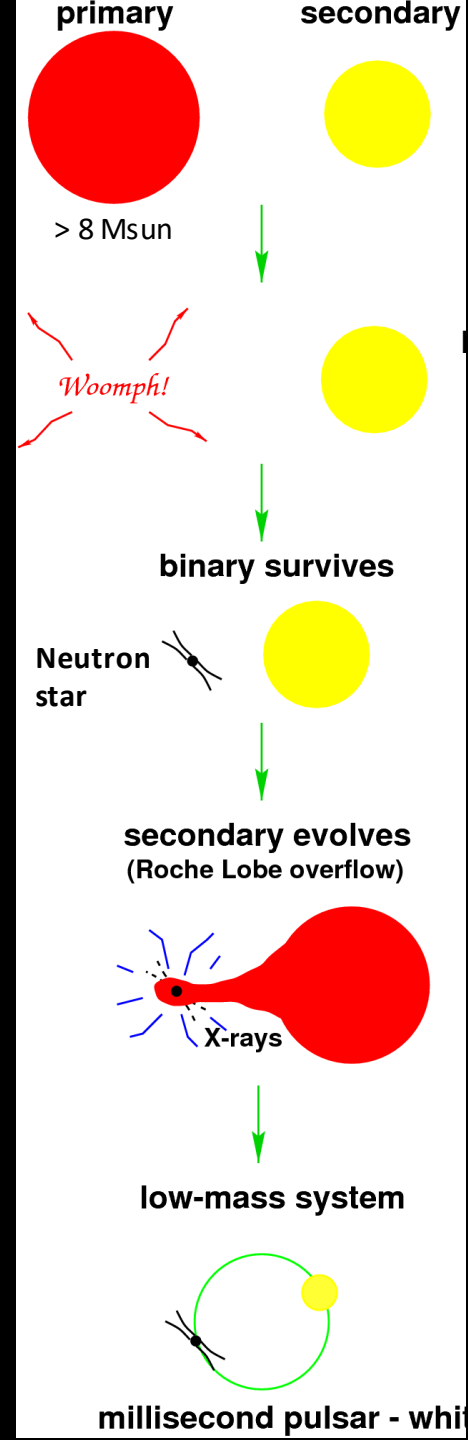
Base	Source	$\log(\mathcal{L}_{\text{Base}})$	$\log(\mathcal{L}_{\text{Base+Source}})$	$\text{TS}_{\text{Source}}$	Number of source parameters	Reference for FB template
baseline	Catenary	-2486188.1	-2486753.1	1130	15	[42]
baseline	Structured FB	-2486188.1	-2487322.3	2268	15	[43]
baseline	Structured FB (Inpainted)	-2486188.1	-2487802.1	3228	15	adapted from [43]

Macias et al. (2019)

Pulsar Recycling Scenario

Recycling of old neutron stars:

- Initially a normal NS, but B-field decays or is buried in the superconducting core (resurface must be stopped)
- ✗ High natal kick velocities might wash out the stellar-bulge vs GCE spatial correlation [e.g., Boodram&Heinke (2022)].
- ✗ Expected a higher number of observed LMXBs in the GC [Haggard+(2017)].



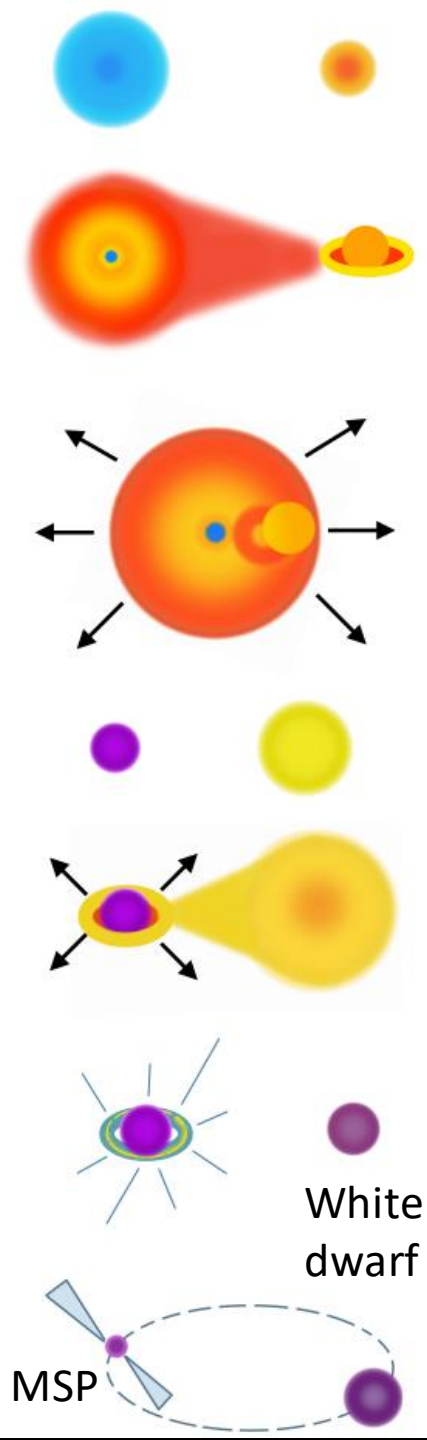


Millisecond pulsars from accretion-induced collapse as the origin of the Galactic Centre gamma-ray excess signal

Gautam, Crocker, Ferrario, Rüter, Ploegg, Gordon, OM (2022)

Accretion-Induced Collapse of White dwarfs:

- Magnetic flux conservation yields the correct B-field.
- Very low or in-existent pulsar natal kicks (consistent with spatial correlation of GCE and stellar bulge).
- Does not generate LMXBs at any stage of the MSPs evolution.



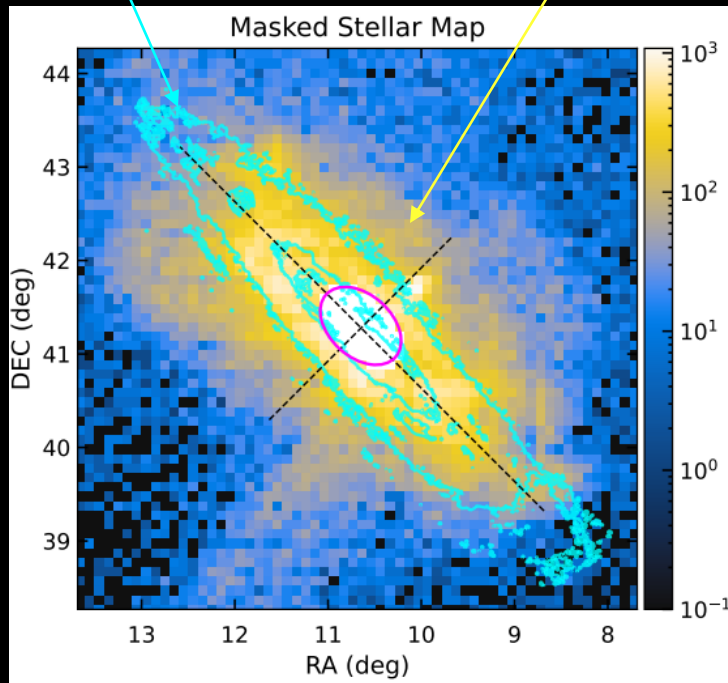
The Andromeda GeV excess

Gamma ray evidence for dark matter annihilations?

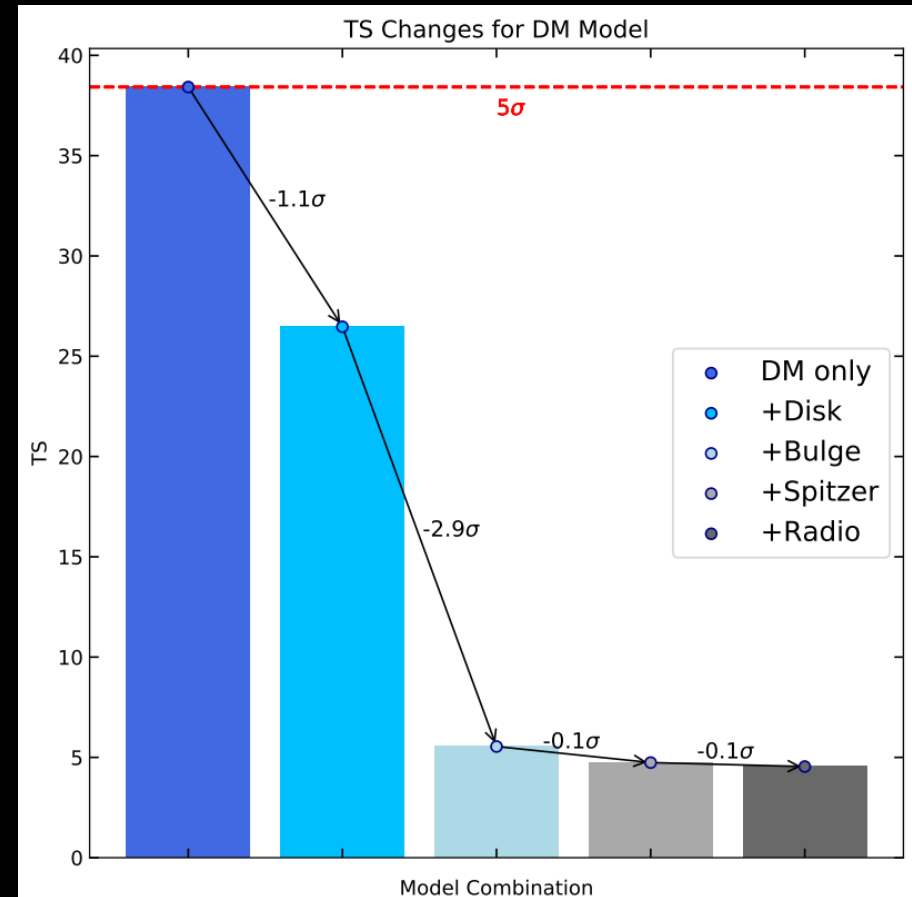
No evidence found once the stellar disk+bulge are included in the fit

Atomic hydrogen

Stars



Zimmer, OM, Ando, Horiuchi, Crocker (2022)

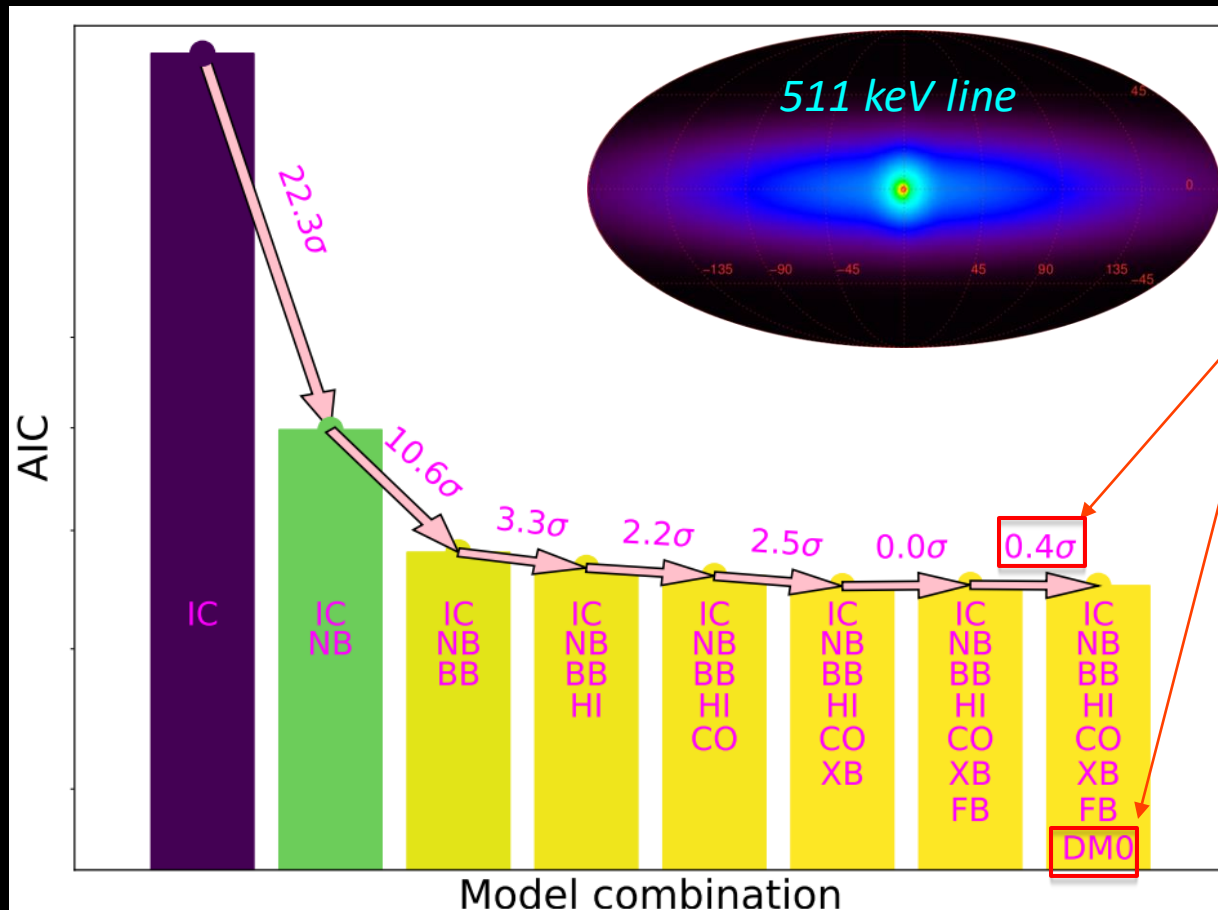


Zimmer, OM, Ando, Horiuchi, Crocker (2022)

Positron Annihilation excess @ GC

Positron annihilation evidence for dark matter annihilations?

No evidence found once the stellar disk+bulge are included in the fit



WITH bulge
Including our bulge model the data no longer needs a dark matter component

Siegert, Crocker, OM, Calore, Horiuchi, Song (2021)